Equilibrium thermodynamics of axion inflation

Yan-Ling Wu,[1,2] Li-Shuang Liu,[1,3] Lin-Hong Sui,[1,4] Yu-Feng Wang,[1,5] Xi-Bin Li,[1,2,*] and Narsu Bai[1,2,†]

[1]*College of Physics and Electronic Information, Inner Mongolia Normal University, 81 Zhaowuda Road, Hohhot, 010022, Inner Mongolia, China*

[2]*Inner Mongolia Key Laboratory for Physics and Chemistry of Functional Materials, Inner Mongolia Normal University, 81 Zhaowuda Road, Hohhot, 010022, Inner Mongolia, China*

[3]*Department of Physics, College of Science, Yanbian University, Yanji, Jilin 133002, China*

[4]*Center for Advanced Optoelectronic Functional Materials Research, and Key Laboratory for UV Emitting Materials and Technology of Ministry of Education, National Demonstration Center for Experimental Physics Education, Northeast Normal University, 5268 Renmin Street, Changchun 130024, China*

[5]*Guangdong Provincial Key Laboratory of Nanophotonic Functional Materials and Devices, School of Information and Optoelectronic Science and Engineering, South China Normal University, Guangzhou 510006, China*

(Received 15 September 2023; accepted 2 November 2023; published 1 December 2023)

Thermal effects from the ensemble average and thermal mass are analyzed in the model of axionic inflaton interacting with U(1) gauge fields through the Chern-Simons coupling $\propto \phi F_{\mu\nu}\tilde{F}^{\mu\nu}/f$ under equilibrium. The ensemble average eliminates the divergence of radiational spectral density. The cosmic temperature is controlled by the parameter $\xi = \dot{\phi}/(2Hf)$ and the renormalization coefficient α_T. It is found that the adiabatic approximation is always corresponding to a slow-roll approximation in the (quasi–)de Sitter universe. The equilibrium condition and backreaction constrain the parameter in a range of $2.47 < \xi < 6.52$, and the axion becomes thermalized if $\xi \simeq 4.0$. Thermal mass leads to the correlation of scalar perturbation and tensor perturbation, which may be a potential method to distinguish different cosmological models. In addition, the tensor-to-scalar ratio is suppressed in a form proportional to H/T if the fields become thermal in the Standard Model. On the other hand, the condition $\xi < 3.0$ is the same as cold inflation, i.e., $r \simeq 16\epsilon$, although thermal effects are taken into consideration.

DOI: 10.1103/PhysRevD.108.123502

I. INTRODUCTION

Inflation theory has successfully explained the primordial power spectrum of cosmic perturbation and is consistent with observations. The most common scenario is an exponential expansion through a cold state with an era of scalar field slowly rolling down a flat potential, and reheating occurs at the end of this stage. But cold inflation does not involve the thermal effects directly, and one of the main tasks of current cosmological research deals with the thermodynamic problems of the early universe. An alternative scheme is the warm inflation model [1,2] in which a dissipation term couples to a thermal bath of particles to realize the transition from potential to radiation. Another objective in warm inflation is the realization of an exponential production of radiation in order to overcome the exponential dilution without spoiling the slow-roll stage. For this purpose, the thermalized axion inflation model is introduced in which the gauge fields A_μ simply couple to an axionlike field ϕ and the gauge fields are considered as the thermal bath [3]. This model of inflation driven by an axionlike particle, often dubbed as natural inflation [4,5], is one of the most well motivated models of inflation to reheat the universe [6,7]. In axion inflation, the flatness of the potential is guaranteed by the shift in symmetry and ensures a periodic potential, where the axion couples with the gauge field through the Chern-Simons coupling $\propto \phi F\tilde{F}/f$ [8].

In axion inflation, a strong production of gauge fields A_μ lies in the constant inflationary field velocity $\dot{\phi}$, or exactly $\xi = \dot{\phi}/(2fH)$. At some extreme conditions with a large enough value of ξ, the production of radiation fields is so large that it backreacts on the background, which is often referred to as the backreaction problem [9–11]. A large ξ can also lead a significant non-Gaussianity of cosmic microwave background in the curvature perturbation in the absence of backreaction [12–14]. Another interesting feature of this coupling is that the inflationary thermodynamics is controlled by the parameter ξ [15,16].

It has been shown in Ref. [15] that there exists an equilibrium state if the ratio $T/H \gg 20$ is analyzed from the Boltzmann equation. Inspired by this work, we continue to focus on the problems of thermodynamics in axion

*lxbbnu@mail.bnu.edu.cn
†nars@imnu.edu.cn

inflation from the Standard Model. In the present paper, the gauge field in the equilibrium state is fully considered as a thermal bath to thermalize the early universe due to the production of radiation from potential. Thermal equilibrium allows a Bose-Einstein distribution, followed by which a radiational spectral density is further obtained. Integrating the spectral density of radiation fields (magnetic and electric fields) over momentum space and combining the Stefan-Boltzmann law yield an equation of cosmic temperature T. Then the adiabaticity could be analytically analyzed by the derivative of the logarithm of T/H with respect to cosmic time, based on which the parameter ξ could also be constrained by the backreaction. The thermal magnetic and electric fields are considered as sources to perturb the cosmic scalar and tensor modes. Green's function method is applied to theoretically calculate the correlation functions of sourced scalar and tensor perturbation, and thus the critical value of ξ thermalizing the axion inflaton is obtained by comparing with the magnitudes of vacuum spectrum. Last, we can also analyze the relation between the tensor-to-scalar ratio and parameter ξ when thermalization happens.

The paper is organized as follows. In Sec. II, the axionic inflationary model is introduced and the solutions of the gauge field in terms of Coulomb functions are obtained. In Sec. III, several problems are analyzed, such as the cosmic temperature, spectral density of radiation (decomposing into magnetic and electric parts), adiabatic approximation, and constraints on parameter ξ. Then, in Sec. IV, treating the thermal magnetic and electric fields as the source to perturb the scalar and tensor modes, the spectrum of sourced scalar and tensor perturbation is obtained; therefore, the suppression of the tensor-to-scalar ratio from thermal effects is shown. Finally, in Sec. V, a brief conclusion of this work and some further discussions about our results are given.

II. MODEL AND EQUATIONS

A. Equation of motion and solution of gauge field

We start from the model described by the following Lagrangian [17]:

$$\frac{\mathcal{L}}{\sqrt{-g}} = \frac{M_p^2 R}{2} - \frac{1}{2}\partial_\mu\phi\partial^\mu\phi - V(\phi) - \frac{1}{4}F_{\mu v}F^{\mu\nu} - \frac{\alpha_c\phi}{4f}F_{\mu v}\tilde{F}^{\mu\nu}, \tag{1}$$

where $M_{\rm p} = (8\pi G)^{-1}$ is the Planck mass, ϕ is the (axion-) inflaton regarded as a scalar field, and $V(\phi)$ is the potential which is most motivated by the natural potential with periodicity:

$$V(\phi) = \Lambda^4\left[1 - \cos\left(\frac{\phi}{f}\right)\right]. \tag{2}$$

The gauge field strength tensor is defined by $F_{\mu\nu} = \partial_\mu A_\nu - \partial_\nu A_\mu$. The U(1) gauge field A_μ couples with inflaton through the Chern-Simons term $\propto \phi F_{\mu v}\tilde{F}^{\mu\nu}$, with the dual tensor $\tilde{F}^{\rho\sigma} = \eta^{\mu\nu\rho\sigma}F_{\mu\nu}/(2\sqrt{-g})$ where $\eta^{\mu\nu\rho\sigma}$ is the Levi-Civita tensor in Minkowski spacetime. The line element in the Friedmann-Robertson-Walker universe reads

$$\begin{aligned} {\rm d}s^2 &= -{\rm d}t^2 + a^2(\delta_{ij} + h_{ij}){\rm d}x^i{\rm d}x^j \\ &= a^2\left[-{\rm d}\tau^2 + (\delta_{ij} + h_{ij}){\rm d}x^i{\rm d}x^j\right], \end{aligned} \tag{3}$$

where t is the cosmic time and τ is the conformal time with derivative relation ${\rm d}t = a{\rm d}\tau$, and h_{ij} is the tensor perturbation. The model we introduced above is about the axion-inflaton ϕ coupled to the gauge field A_μ directly. A more general model is ϕ couples to A_μ indirectly via a spectator field σ [18]. However, in this paper, we mainly attempt to show the effects from the thermalized gauge field, instead of the model itself.

The equation of motion of 4-potential A_μ is obtained by varying the action with respect to A_μ:

$$\frac{1}{\sqrt{-g}}\frac{\partial}{\partial x^\nu}\left[\sqrt{-g}\left(g^{\mu\alpha}g^{v\beta}F_{\alpha\beta} + \frac{\alpha_c\phi}{2\sqrt{-g}}\eta^{\mu v\alpha\beta}F_{\alpha\beta}\right)\right] = 0. \tag{4}$$

This equation is convenient to work in the frame of Coulomb gauge $A^0 = 0$ and $\partial^i A_i = 0$; therefore, it yields

$$\left(\frac{\partial^2}{\partial\tau^2} - a^2\partial_i\partial^i - \alpha_c\frac{a\dot{\phi}}{f}\nabla\times\right)\mathbf{A}(\mathbf{x},\tau) = 0, \tag{5}$$

where the dot $\dot{}$ denotes the derivative with respect to cosmic time t. To quantize the electric and magnetic (EM) fields, the conjugate momentum $\Pi_i = \delta\mathcal{L}/\delta\dot{A}_i$ of the field A_i is introduced following the canonical quantization condition

$$[A_i(\mathbf{x}), \Pi_j(\mathbf{y})] = {\rm i}\int\frac{{\rm d}^3p}{(2\pi)^3}{\rm e}^{\mathbf{k}\cdot(\mathbf{x}-\mathbf{y})}P_{ij}(\mathbf{k}), \tag{6}$$

where the projection tensor $P_{ij}(\mathbf{k}) = \delta_{ij} - k_ik_j/k^2$ is to ensure the Coulomb gauge condition. The gauge field $A_i(\mathbf{x})$ is quantized by the momentum space operator via Fourier transform

$$\begin{aligned} \hat{A}_i(\mathbf{x},\tau) &= \int\frac{{\rm d}^3k}{(2\pi)^3}\sum_{\lambda=\pm}\left[\epsilon_i^\lambda(\mathbf{k})\bar{A}_\lambda(\mathbf{k},\tau)\hat{a}_\lambda(\mathbf{k}){\rm e}^{{\rm i}\mathbf{k}\cdot\mathbf{x}} + \epsilon_i^{\lambda*}(\mathbf{k})\bar{A}_\lambda^*(\mathbf{k},\tau)\hat{a}_\lambda^\dagger(\mathbf{k}){\rm e}^{-{\rm i}\mathbf{k}\cdot\mathbf{x}}\right] \\ &= \int\frac{{\rm d}^3k}{(2\pi)^3}\sum_{\lambda=\pm}\epsilon_i^\lambda(\mathbf{k}){\rm e}^{{\rm i}\mathbf{k}\cdot\mathbf{x}}\left[\bar{A}_\lambda(\mathbf{k},\tau)\hat{a}_\lambda(\mathbf{k}) + \bar{A}_\lambda^*(-\mathbf{k},\tau)\hat{a}_\lambda^\dagger(-\mathbf{k})\right], \end{aligned} \tag{7}$$

where $\epsilon_i^\pm(\mathbf{k})$ is the polarization vectors that relate to the orthonormal 3-vector in flat space $\hat{\epsilon}_i^\alpha(\mathbf{k})$:

$$\epsilon_{\pm}^{i}=\frac{\hat{\epsilon}_{\pm}^{i}}{a},\quad \epsilon_{3}^{i}=\frac{\hat{k}}{a},\quad \text{with dual vector } \epsilon_{i}^{\alpha}=a\hat{\epsilon}_{i}^{\alpha}\quad(\alpha=\pm,3). \tag{8}$$

In Eq. (7), $\hat{a}_{\lambda}(\mathbf{k})/\hat{a}_{\lambda}^{\dagger}(\mathbf{k})$ is the annihilation/creation operator satisfying commutation relation

$$\left[\hat{a}_{\lambda}(\mathbf{k}),\hat{a}_{\lambda'}^{\dagger}(\mathbf{k}')\right]=(2\pi)^3\delta_{\lambda\lambda'}\delta^3(\mathbf{k}+\mathbf{k}'). \tag{9}$$

Define the variable $A_\lambda = a\bar{A}_\lambda$ and substitute Eq. (7) into Eq. (4), and then we obtain the equation of polarization vector of 4-potential in momentum space

$$A_{\pm}''+k^2A_{\pm}\pm\frac{2k\xi}{\tau}A_{\pm}=0, \tag{10}$$

with $\xi=\alpha_c\dot{\phi}/(2Hf)$ and prime $'$ denoting the derivative respect to conformal time τ. In the process of deriving the above equation, we have used the properties (B2) of polarization vectors. The approximate equality in Eq. (10) arises due to the assumption that the dimensionless measure of field velocity ξ evolves adiabatically, i.e., $\dot{\xi}/\xi H\ll 1$.

However, Eq. (10) is the equation of motion of the gauge field without taking thermalization into account. As an important modification to Eq. (10), when thermalization happens, the gauge field develops a thermal mass $m_T=\alpha_T T$ via one-loop thermal correction [7,19]. Thus Eq. (10) becomes

$$\left(\frac{\partial^2}{\partial z^2}+1\mp\frac{2\xi}{z}+\frac{\alpha_T^2T^2}{H^2z^2}\right)A_{\pm}=0 \tag{11}$$

with $z=-k\tau$. Equation (11) is an equation in the form of Coulomb function

$$\left(\frac{\partial^2}{\partial z^2}+1-\frac{2\xi}{z}-\frac{\ell(\ell+1)}{z^2}\right)\psi=0, \tag{12}$$

where ℓ is obtained by satisfying the equation $\ell(\ell+1)=-\mu^2$, with $\mu^2=\alpha_T^2T^2/H^2$. ℓ has two solutions, and we take the one

$$\ell=\frac{-1+\sqrt{1-4\mu^2}}{2} \tag{13}$$

as the index of two linearly independent Coulomb functions $H_{\ell}^{(\pm)}$, because solutions $H_{\ell'}^{(\pm)}$, with $\ell'=(-1-\sqrt{1-4\mu^2})/2$, can be linearly represented from $H_{\ell}^{(\pm)}$. Obviously the relation between $4\mu^2$ and 1 determines the solution of ℓ to be a real number or a complex number. The canonical relation (6) and the Bunch-Davies vacuum in the subhorizon limit $A_{\pm}\to(2k)^{-1/2}\mathrm{e}^{-\mathrm{i}k\tau}$ as $-k\tau\to\infty$ lead the solution of Eq. (11) on a superhorizon scale approximately

$$\begin{aligned}A_{\pm}&=\frac{1}{\sqrt{2k}}\exp\mathrm{i}[\pm\xi\ln(-2k\tau)+\ell\pi/2-\sigma_\ell(\pm\xi)]H_{\ell}^{(\pm)}(\xi,\tau)\\&\approx\frac{1}{\sqrt{2k}}\exp\mathrm{i}[\pm\xi\ln(-2k\tau)+\ell\pi/2-\sigma_\ell(\pm\xi)]\times\begin{cases}\frac{\mathrm{i}(-k\tau)^{-\ell}}{(2\ell+1)C_\ell(\pm\xi)}, & 4\mu^2<1\\ \left(\frac{\pi}{\exp(\pm2\pi\xi)+1}\right)^{\frac{1}{2}}(-k\tau)^{\frac{1}{2}}\left[1+\frac{\exp(\pm2\pi\xi)+1}{\mathrm{i}\pi}\ln(-k\tau)\right], & 4\mu^2=1\\ C_\ell(\pm\xi)(-k\tau)^{\ell+1}+\frac{(-k\tau)^{-\ell}}{(2\ell+1)C_\ell(\pm\xi)}, & 4\mu^2>1\end{cases}\end{aligned} \tag{14}$$

The definitions of $\sigma_\ell(\xi)$, $H_{\ell}^{(\pm)}(\xi,\tau)$, $C_\ell(\xi)$ and the properties of the Coulomb function are listed in Appendix A. In addition, the special value $\mu=1/2$ has only a mathematical specificity instead of a physical meaning, and it does not lead to a special result, so in the following sections we ignored it.

III. SPECTRUM OF GAUGE FIELD

A. Relevant definitions

The definitions of "electric" and "magnetic" fields from gauge field strength tensor $F_{\mu\nu}$ are expressed as $E_\mu=u^\nu F_{\mu\nu}$ and $B_\mu=u^\nu\tilde{F}_{\mu\nu}$. For the observer $u^\mu=(1/a,0,0,0)$, the electromagnetic fields of the spatial component are defined with an extra inverse scale factor a^{-1}:

$$\hat{E}_i=-\frac{1}{a^2}\hat{A}_i',\qquad \hat{B}_i=\frac{1}{a^2}\eta_{ijk}\delta^{jm}\delta^{kn}\partial_m\hat{A}_n, \tag{15}$$

or in momentum space

$$\begin{aligned}\hat{E}_i(\mathbf{k},\tau)&=-\frac{1}{a^2}\hat{A}_i',\\ \hat{B}_i(\mathbf{k},\tau)&=\mathrm{i}\frac{1}{a^2}\eta_{ijl}\delta^{jm}\delta^{ln}k_m\hat{A}_n(\mathbf{k},\tau).\end{aligned} \tag{16}$$

Definitions (15) and (16) make it convenient to deal with the contraction, for example, $B_iB^i=\delta^{ij}B_iB_j=B_iB_i$. So in the following sections, except for special instructions, the vectors or tensors under contraction are dealt in Minkowski spacetime.

The energy density of component X is defined as

$$\rho_X = \int \mathrm{d}\ln k \frac{\mathrm{d}\rho_X(k,\tau)}{\mathrm{d}\ln k} = \int \frac{\mathrm{d}k}{k}\frac{k^3}{2\pi^2}\int \mathrm{d}^3k' \langle X(\mathbf{k},\tau)X(\mathbf{k}',\tau)\rangle. \quad (17)$$

Here the component X may be a scalar perturbation, a tensor perturbation, a radiation field, an electric field, or a magnetic field. The spectrum density in terms of a two-point correlation function reads

$$\frac{\mathrm{d}\rho_X(k,\tau)}{\mathrm{d}\ln k} \equiv \frac{k^3}{2\pi^2}\int \mathrm{d}^3k' \langle X(\mathbf{k},\tau)X(\mathbf{k}',\tau)\rangle. \quad (18)$$

Before we get the energy density of the radiation field, it is necessary to introduce the energy momentum tensor of the electric and magnetic fields [20]:

$$T_{\mu\nu} = -\frac{2}{\sqrt{-g}}\frac{\delta\sqrt{-g}\mathcal{L}}{\delta g^{\mu\nu}} = g^{\alpha\beta}F_{\mu\alpha}F^{\nu\beta} - \frac{1}{4}g_{\mu\nu}F_{\alpha\beta}F^{\alpha\beta}, \quad (19)$$

with a 00 component and a ij component, respectively,

$$\langle T_{00}\rangle = \rho_B + \rho_E = \frac{1}{2}\langle B^iB_i + E^iE_i\rangle(\mathbf{x},\tau),$$
$$T_{ij} = B_iB_j + E_iE_j - \frac{1}{2}g_{ij}(B_mB^m + E_mE^m). \quad (20)$$

We should point out that $\langle\cdots\rangle$ means the ensemble average

$$\langle \hat{A}\,\hat{B}\rangle = \mathrm{tr}[:\hat{A}\,\hat{B}:], \quad (21)$$

where $:\cdots:$ represents the normal product meaning that the annihilation operator always locates at the right-hand side of the creation operator. Especially, the ensemble average of the combination of the creation and annihilation operators is

$$\left\langle \hat{a}^\dagger_\lambda(\mathbf{k})\hat{a}_{\lambda'}(\mathbf{k}')\right\rangle = (2\pi)^3\delta_{\lambda\lambda}\delta^3(\mathbf{k}+\mathbf{k}')\cdot n_{\mathrm{B}}(\omega_k/aT). \quad (22)$$

The equation above involves a Bose-Einstein distribution function at equilibrium defined as [15,21]

$$n_{\mathrm{B}}(\omega_k/aT) = (\mathrm{e}^{\frac{\omega_k}{aT}} - 1)^{-1}, \quad (23)$$

where T denotes the cosmic temperature during inflation and $\omega_k = \sqrt{k^2 + a^2m_T^2}$ is the comoving energy of a particle. Note that ω_k/a is the physical wave number corresponding to the energy of the gauged particle by the timing constant $\hbar c$. It should be emphasized that the results above are based on the (near) equilibrium hypothesis, which will be discussed in detail subsequently. This hypothesis is based on the fact that scattering rates involving gauge fields can become larger than the expansion rate H and create a thermal bath of particles of temperature T during inflation.

B. Spectral electromagnetic energy density

The two-point correlation function of magnetic field in momentum space is defined as

$$\mathcal{P}_{B,ij}(\mathbf{k},\mathbf{k}',\tau) = \langle \hat{B}_i(\mathbf{k},\tau)\hat{B}_j(\mathbf{k}',\tau)\rangle = \frac{(2\pi)^3}{a^4}\delta^3(\mathbf{k}+\mathbf{k}')\sum_{\lambda=\pm}\sum_{l_1}\sum_{l_2m_1m_2}\eta_{il_1m_1}\eta_{jl_2m_2}k^{l_1}k^{l_2} \cdot\epsilon_\lambda^{m_1}(\epsilon_\lambda^{m_2})^* A_\lambda(\mathbf{k},\tau)A^*_\lambda(\mathbf{k},\tau)n_{\mathrm{B}}\left(\frac{\omega_k}{aT}\right). \quad (24)$$

Applying Eq. (B6) in Appendix B, then Eq. (24) becomes

$$\mathcal{P}_{B,ij}(\mathbf{k},\mathbf{k}',\tau) = \frac{(2\pi)^3}{a^4}\delta^3(\mathbf{k}+\mathbf{k}')n_{\mathrm{B}}(\omega_k/aT)(-\tau) \cdot\Big[(\delta_{ij} - \hat{k}_i\hat{k}_j)k^2P_B(k,\tau) + \mathrm{i}\eta_{ikm}\hat{k}^mk^2S_B(k,\tau)\Big], \quad (25)$$

where $\hat{k}_i = k_i/k$ is the unit vector parallel to k_i, the dimensionless variables P_B is about the symmetric part, and S_B is about the antisymmetric part:

$$P_B(k,\tau) = \frac{1}{-\tau}(|A_+|^2 + |A_-|^2),$$
$$S_B(k,\tau) = \frac{1}{-\tau}(|A_+|^2 - |A_-|^2). \quad (26)$$

Equation (B4) has been used in the derivation of Eq. (25). Based on the expression in Eq. (14), we have the approximate expressions of P_B and S_B,

$$P_B/S_B(k,\tau) \approx \frac{1}{-k\tau}\times\begin{cases}\frac{(-k\tau)^{-2\ell}\Gamma^2(2\ell+2)}{(2\ell+1)^2\cdot 2^{2\ell}}\left[\frac{\mathrm{e}^{\pi\xi}}{|\Gamma(\ell+1+\mathrm{i}\xi)|^2} \pm \frac{\mathrm{e}^{-\pi\xi}}{|\Gamma(\ell+1-\mathrm{i}\xi)|^2}\right], & 4\mu^2 < 1\\ (-k\tau)\left|\frac{\Gamma(2\ell+2)\cdot\exp(\mathrm{i}\ell\pi/2)}{(2\ell+1)\cdot 2^\ell}\right|^2\left[\frac{\mathrm{e}^{\pi\xi}}{|\Gamma(\ell+1+\mathrm{i}\xi)|^2} \pm \frac{\mathrm{e}^{-\pi\xi}}{|\Gamma(\ell+1-\mathrm{i}\xi)|^2}\right], & 4\mu^2 > 1\end{cases}. \quad (27)$$

It is obvious that S_B vanishes if $\xi = 0$.

Based on Eq. (B6), the two-point correlation function of the electric field in momentum space reads

$$\begin{aligned}\mathcal{P}_{E,ij}(\mathbf{k},\mathbf{k}',\tau) &= \langle \hat{E}_i(\mathbf{k},\tau)\hat{E}_j(\mathbf{k}',\tau)\rangle \\ &= \frac{(2\pi)^3}{a^4}\delta^3(\mathbf{k}+\mathbf{k}')n_{\mathrm{B}}(\omega_k/aT)\cdot(-\tau)[(\delta_{ij}-\hat{k}_i\hat{k}_j)k^2P_E(k,\tau)-\mathrm{i}\eta_{ikm}\hat{k}^m k^2 S_E(k,\tau)],\end{aligned} \tag{28}$$

with

$$\begin{aligned}P_E/S_E(k,\tau) &= \frac{1}{k^2(-\tau)}[|(A_+)'|^2 \pm |(A_-)'|^2] \approx \frac{1}{-k\tau} \\ &\times \begin{cases} (-k\tau)^{-2\ell}\frac{(1-\ell)^2\Gamma^2(2\ell+2)}{(2\ell+1)^2\cdot 2^{2\ell}}\left[\frac{\mathrm{e}^{\pi\xi}}{|\Gamma(\ell+1+\mathrm{i}\xi)|^2}\pm\frac{\mathrm{e}^{-\pi\xi}}{|\Gamma(\ell+1-\mathrm{i}\xi)|^2}\right], & 4\mu^2<1 \\ (-k\tau)\left|\frac{(1-\ell)\Gamma(2\ell+2)\cdot\exp(\mathrm{i}\ell\pi/2)}{(2\ell+1)\cdot 2^{\ell}}\right|^2\left[\frac{\mathrm{e}^{\pi\xi}}{|\Gamma(\ell+1+\mathrm{i}\xi)|^2}\pm\frac{\mathrm{e}^{-\pi\xi}}{|\Gamma(\ell+1-\mathrm{i}\xi)|^2}\right]. & 4\mu^2>1 \end{cases}.\end{aligned} \tag{29}$$

The projector tensor $\delta_{ij}-\hat{k}_i\hat{k}_j$ in Eq. (28) comes from the Coulomb gauge $k^iE_i=0$.

Similarly, the two-point correlation function of the crossing term between electric and magnetic fields in momentum space is

$$\begin{aligned}\mathcal{P}_{C,ij}(\mathbf{k},\mathbf{k}',\tau) &= \langle \hat{E}_i(\mathbf{k},\tau)\hat{B}_j(\mathbf{k}',\tau)\rangle \\ &= \frac{(2\pi)^3}{a^4}\delta^3(\mathbf{k}-\mathbf{k}')n_{\mathrm{B}}(\omega_k/aT)\cdot(-\tau)\times\sum_\lambda(-\mathrm{i})\eta_{jml}k^l\epsilon_\lambda^i(\epsilon_\lambda^m)^*A'_\lambda(\mathbf{k},\tau)A^*_\lambda(\mathbf{k},\tau) \\ &= \frac{(2\pi)^3}{a^4}\delta^3(\mathbf{k}-\mathbf{k}')n_{\mathrm{B}}(\omega_k/aT)(-\mathrm{i})\eta_{jml}k^l\left[\delta^{im}kP_C(\mathbf{k},\tau,\tau')+(\sigma_2)^{im}kS_C(\mathbf{k}_p,\tau,\tau')\right] \\ &= \frac{(2\pi)^3}{a^4}\delta^3(\mathbf{k}-\mathbf{k}')n_{\mathrm{B}}(\omega_k/aT)\left[-(\delta_{ij}-\hat{k}_i\hat{k}_j)k^2S_C(\mathbf{k}_p,\tau,\tau')+\mathrm{i}\eta_{ijm}\hat{k}^mk^2P_C(\mathbf{k}_p,\tau,\tau')\right],\end{aligned} \tag{30}$$

with dimensionless variables

$$\begin{aligned}P_C/S_C(k,\tau) &= \frac{1}{-2k\tau}\frac{\partial}{\partial\tau}(|A_+|^2\pm|A_-|^2) \approx \frac{1}{-k\tau} \\ &\times \begin{cases} (-k\tau)^{-2\ell}\frac{(1-\ell)\Gamma^2(2\ell+2)}{(2\ell+1)^2\cdot 2^{2\ell}}\left[\frac{\mathrm{e}^{\pi\xi}}{|\Gamma(\ell+1+\mathrm{i}\xi)|^2}\pm\frac{\mathrm{e}^{-\pi\xi}}{|\Gamma(\ell+1-\mathrm{i}\xi)|^2}\right], & 4\mu^2<1 \\ (-k\tau)\cdot|1-\ell|\cdot\left|\frac{\Gamma(2\ell+2)\cdot\exp(\mathrm{i}\ell\pi/2)}{(2\ell+1)\cdot 2^{\ell}}\right|^2\left[\frac{\mathrm{e}^{\pi\xi}}{|\Gamma(\ell+1+\mathrm{i}\xi)|^2}\pm\frac{\mathrm{e}^{-\pi\xi}}{|\Gamma(\ell+1-\mathrm{i}\xi)|^2}\right]. & 4\mu^2>1 \end{cases}.\end{aligned} \tag{31}$$

Another crossing correlation function of electric and magnetic fields is $\langle\hat{B}_i(\mathbf{k},\tau)\hat{E}_j(\mathbf{k}',\tau)\rangle=\langle\hat{E}_i(\mathbf{k},\tau)\hat{B}_j(\mathbf{k}',\tau)\rangle^*$.

It is seen that it emerges as a regular and orderly form of electromagnetic two-point correlation functions due to definitions (15). These approximations will be used to calculate the spectra in the next section.

C. Numerical results

Because of the analytical expressions of two-point correlation functions of electric, magnetic, and crossing fields obtained in Sec. III B and 4-potential A_μ in Eq. (14), the spectral density and polarized density of the magnetic field can be expressed as

$$\begin{aligned}\frac{\mathrm{d}\rho_B(k,\tau)}{\mathrm{d}\ln k} &= \delta_{ij}\frac{k^3}{2\pi^2}\int\mathrm{d}^3k'\mathcal{P}_{B,ij}(\mathbf{k},\mathbf{k}',\tau) \\ &= 2\pi H^4\left(\frac{k}{aH}\right)^5 n_{\mathrm{B}}\left(\frac{\omega_k}{aT}\right)P_B\left(\frac{k}{aH}\right), \\ \frac{\mathrm{d}s_B(k,\tau)}{\mathrm{d}\ln k} &= -\mathrm{i}\eta_{ijn}\hat{k}^n\frac{k^3}{2\pi^2}\int\mathrm{d}^3k'\mathcal{P}_{B,ij}(\mathbf{k},\mathbf{k}',\tau) \\ &= 2\pi H^4\left(\frac{k}{aH}\right)^5 n_{\mathrm{B}}\left(\frac{\omega_k}{aT}\right)S_B\left(\frac{k}{aH}\right).\end{aligned} \tag{32}$$

P_B and S_B are defined in Eq. (26), and these expressions also apply to electric field E and crossing term C.

1. Spectral density and polarized density

In the case of the Standard Model, it gives $\alpha_T^2 \simeq 0.3$ at the energies of around 10^{14} GeV. The typical scale $k_* = a_* H_*$ at the crossing horizon is set to 0.05 Mpc^{-1}. The spectral density and polarized density of the magnetic field, electric field, cross term, and radiation field in terms of k/k_* with $\xi = 0.1$ are plotted in Fig. 1, and the spectral density and polarized density of the radiation field with $\xi = 0.2$ and $\xi = 0.3$ are plotted in Fig. 2. Here the spectral density of radiation means the sum of magnetic and electric spectral density, and it also applies to the polarized density. The numerical results are obtained from the analytical expressions of 4-potentials A_μ in terms of the Whittaker function in Eq. (A10). Lines with different styles stand for the conditions with different values of T/H, and the black lines represent the spectral densities while the red lines represent the polarized densities. The lines with $(T/H)^2 = 5/6$ represent the critical condition by $4\mu^2 = 1$. The profiles of spectral and polarized density with $T/H \gg 1$ are similar to those with $T/H \sim 1$, and the peaks always locate at $k/k_* > 1$, but the amplitudes are much larger, so we do not plot these cases.

Figures 1 and 2 show that the spectrums vanish as k goes to infinity, meaning the problem of ultraviolet divergence no longer exists, which is often suffered in a zero temperature condition [22]. The radiation energy density is mainly contributed from the region inside the horizon. The spectrums show the sharps similar to that in a black body, which is consistent with observations on a cosmic microwave background. The magnetic field and the electric field contribute the opposite polarized density (noting the positive and negative symbols in Fig. 1) due to the curl asymmetry of the electric and magnetic fields. The peak of the polarized density of radiation almost locates at the scale of horizon but is a little smaller than that. This phenomenon may come from the suppression on the horizon by the scattering of the gauge field with an axionic inflaton. Based on the discussions above, it suggests that the cosmological horizon is not only important for dynamics of the scalar field, but also is important for thermodynamic problems. In addition, the last panel in Fig. 1 and the panels in Fig. 2 indicate that a large value ξ means a higher energy density and a stronger polarization of radiation.

2. Cosmic temperature

From the definition of spectral density, it is easy to test a total form of the black body spectrum when $\alpha_C = \alpha_T = 0$ (indicating $\xi = \ell = 0$):

$$\frac{\mathrm{d}\rho_r}{\mathrm{d}\ln k} = 4\pi H^4 \left(\frac{k}{aH}\right)^4 \frac{1}{\exp\left(\frac{k}{aH}\frac{H}{T}\right) - 1} \tag{33}$$

and $\mathrm{d}s_r/\mathrm{d}\ln k = 0$. The integral over logarithmic momentum space corresponds to the Stefan-Boltzmann law $\rho_r = \frac{\pi^2}{30} g_* T^4$, where g_* characterizes the number of

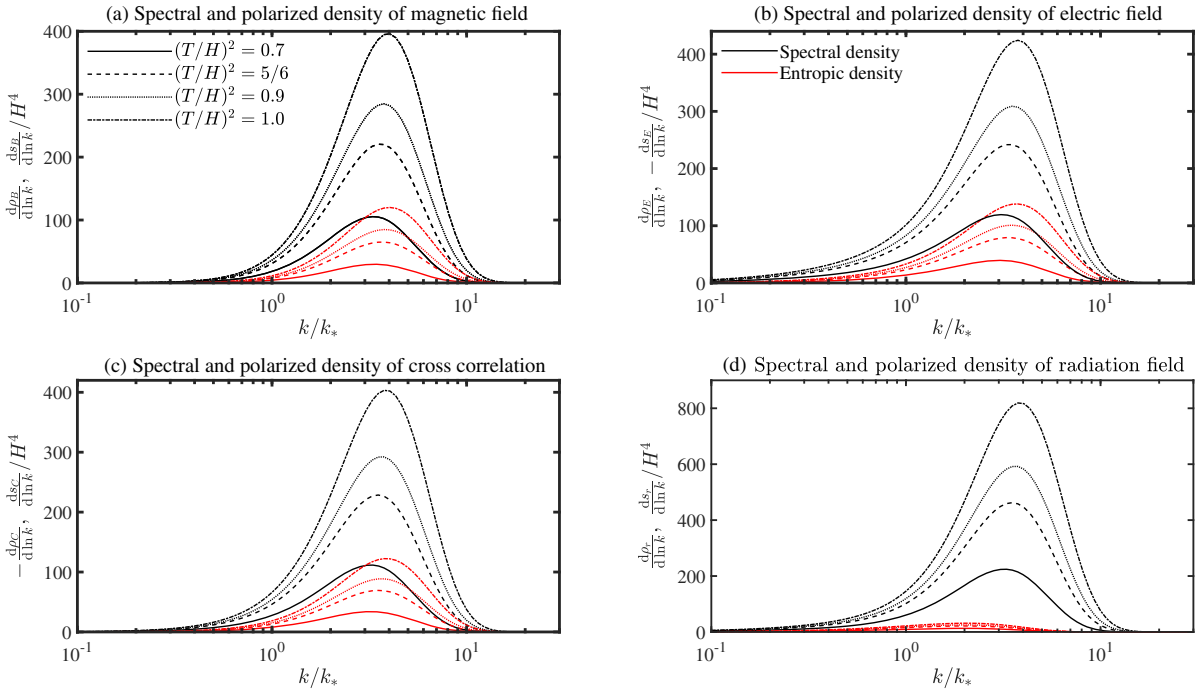

FIG. 1. The spectral density and polarized density of (a) magnetic field, (b) electric field, (c) cross-correlation, and (d) radiation field by setting $\xi = 0.1$. The lines in each panel with different styles represent the density with different cosmic temperature; the black and red lines represent the spectral density and polarized density, respectively.

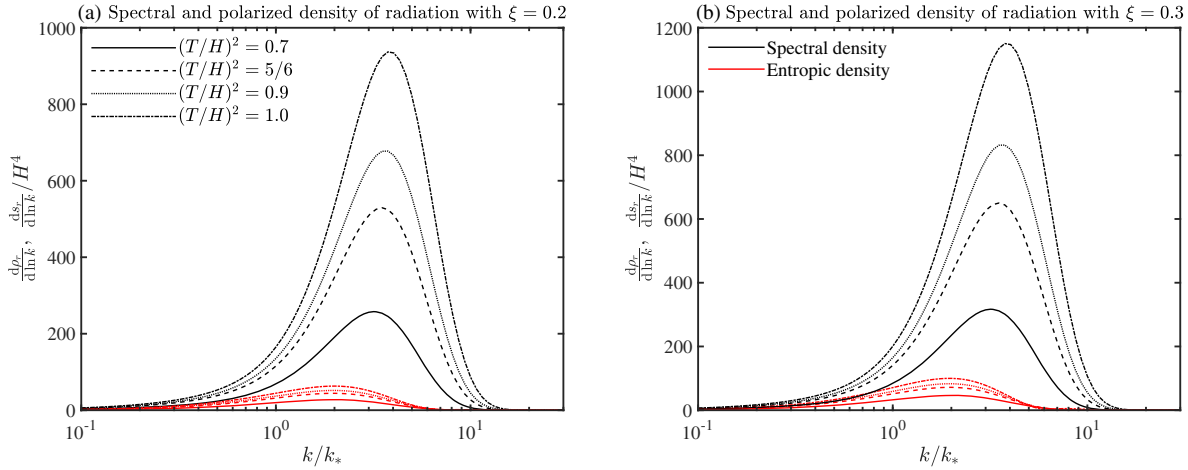

FIG. 2. The spectral density and polarized density of the radiation field with (a) $\xi = 0.2$ and (b) $\xi = 0.3$.

relativistic particle degrees of freedom. Then applying the formula about energy density of radiation in Eq. (20), we obtain the equation

$$\rho_r = \int \mathrm{d}\ln k \left(\frac{\mathrm{d}\rho_B}{\mathrm{d}\ln k} + \frac{\mathrm{d}\rho_E}{\mathrm{d}\ln k} \right) = \frac{\pi^2}{30} g_* T^4. \quad (34)$$

It reveals that the equation above is about the variable T/H and parameters ξ and α_T, which may only be solved by a numerical method. To obtain the solution of T/H as accurately as possible, the exact expressions of gauge field $A_\pm$ in (14) in terms of Coulomb functions or Whittaker functions are used. The relation of the ratio of cosmic temperature to cosmic Hubble parameter T/H and parameter ξ, α_T is shown in Fig. 3. The parameters are set as $\Lambda \sim 10^{-3} M_\mathrm{p}$, $f \sim M_\mathrm{p}$ [6], and $g_* = 106.75$ [23]. We see that the ratio T/H is not sensitive on ξ (or α_C) when smaller than a critical value and a stronger coupling constant of α_T means a higher cosmic temperature. This is because a stronger interaction means a more intense conversion process from potential to radiation, which makes it possible to hold a higher temperature. On the other hand, larger values of α_T decrease the cosmic temperature. This may come from a sufficiently heavy thermal mass $m_T = \alpha_T T$ that suppresses the scattering between the scalar field and the gauge field. So this is to maintain the temperature in an appropriate range.

Another interesting phenomenon is that inflationary temperature T never appears alone, but in the form of a ratio to Hubble parameter H. So inflationary thermodynamics is a physical process competing with geometric dynamics, which is also mentioned in Ref. [16].

The equilibrium state requires $T/H > 20$ [15], which leads the first condition $\xi > 2.47$ at $\alpha_T^2 \simeq 0.3$.

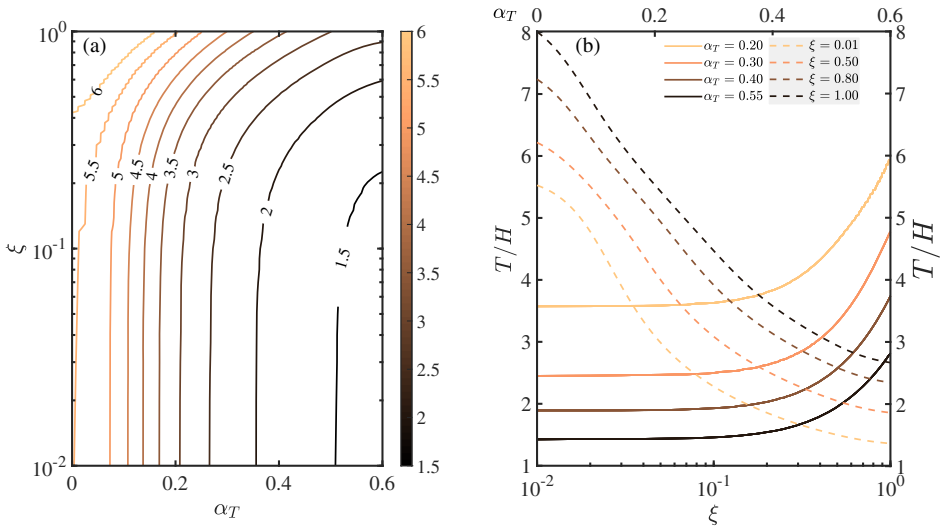

FIG. 3. (a) Contours of the ratio of cosmic temperature to Hubble parameter T/H in the $\xi - \alpha_T$ plane. (b) Relation between T/H and ξ (solid lines with different values of α_T scaled by the bottom axis) and α_T (dashed lines with different values of ξ scaled by the top axis).

D. Adiabatic approximation

As seen in the previous section, the adiabatic approximation holds during inflation since the cosmic temperature is nearly constant, which may be verified by the relation $|\frac{\dot{T}}{HT}| \ll 1$. The derivative of the logarithm of T/H over cosmic time t reads

$$\frac{1}{H}\frac{\mathrm{d}\ln T/H}{\mathrm{d}t} = \frac{\dot{T}}{HT} + \varepsilon. \tag{35}$$

Another way to obtain $\ln(T/H)$ is from Eq. (34) which is approximately analytically expressed from $\mathrm{d}\rho_B/\mathrm{d}\ln k$ and $\mathrm{d}\rho_E/\mathrm{d}\ln k$. As mentioned previously, equilibrium condition $T/H > 20$ yields the relation $4\mu^2 \gg 1$ or $\ell \simeq -1/2 + \mathrm{i}\mu$. Thus, the adiabatic parameter with $4\mu^2 \gg 1$ can be approximately expressed as

$$\delta_T = -\frac{\dot{T}}{HT} \simeq \frac{H^{-1}\dot{\xi}[\pi - \mathrm{i}\psi(\ell+1+\mathrm{i}\xi) + \mathrm{c.c.}]}{F(\ell)\alpha_T \frac{T}{H}} + \varepsilon \tag{36}$$

with

$$F(\ell) = \left[\frac{\mathrm{i}}{\ell(\ell+1)} + \mathrm{i}\psi(2\ell+2) - \pi - \mathrm{i}\psi(\ell+1+\mathrm{i}\xi)\right] + \mathrm{c.c.} + \mathcal{O}(\alpha_T^2), \tag{37}$$

where $\psi(z)$ is the digamma function [24] and c.c. denotes the complex conjugation. It is obvious $F(\ell)$ is a function dependent on T/H, and thus the adiabatic approximation $|\frac{\dot{T}}{HT}| \ll 1$ holds only if $H^{-1}\dot{\xi} \ll 1$ which is equivalent to the slow-roll approximation. So an intimate relation between inflationary adiabatic approximation and inflationary slow-roll approximation is shown. It also suggests that adiabatic approximation naturally holds in the frame of the axionic inflationary model. Figure 4 shows the evolutionary trends of adiabatic parameter δ_T as a function of the e-folding number with $T/H = 25$ and the same combination of parameters as that in Sec. III C 2.

E. Constraints from backreaction

The suffering on the backreaction problem often appears in the case of a gauge field with zero temperature, which may be overcome by an axionic inflaton dependent model named the Ratra model [25]. This problem mainly comes from the divergence of the ultraviolet band $k \to \infty$, and a conventional method to deal with it is setting a cutoff on an ultraviolet band. In our analysis, the cutoff is removed by introducing the ensemble average. The avoidance of the backreaction problem requires energy density of radiation ρ_r and energy density of inflaton ρ_ϕ to hold the condition $\rho_r \ll \rho_\phi \approx V(\phi)$ during inflation, or exactly

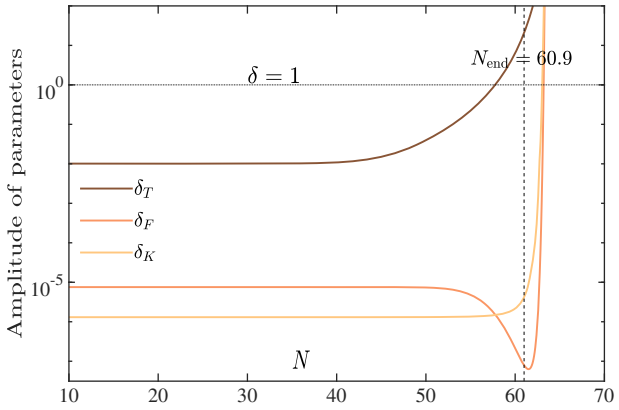

FIG. 4. Curves of δ_T, δ_F, and δ_K with equilibrium condition $T/H = 25$. The horizontal dotted line is the critical value of the parameters with a unit value, and the vertical dashed line is the e-folding number at the end of inflation quantified as slow-roll parameter $\varepsilon = 1$.

$$\delta_F = \frac{\rho_r}{\rho_\phi} \simeq \frac{\rho_B + \rho_E}{3H^2M_{\mathrm{p}}^2} = \frac{\pi^2 g_*}{30}\frac{T^4}{H^4}\frac{\Lambda^4}{9M_{\mathrm{p}}^4}\left[1 - \cos\left(\frac{\phi}{f}\right)\right] \ll 1, \tag{38}$$

where the natural potential (2) is applied. If $\delta_F \geq 1$, it assumes that the cosmic domination by inflaton is broken down and the universe is dominated by radiation. Another parameter is the ratio of the source term to the Hubble friction term

$$\delta_K = \left|\frac{\rho_{BE}/f}{3H\dot{\phi}}\right| \ll 1, \tag{39}$$

which is used to characterize the instability of the inflaton field. If $\delta_K \geq 1$, it means a suppression of the gauge amplification. So, it requires the conditions $\delta_{\mathrm{F}} < 1$ and $\delta_K < 1$ during the inflationary era due to the consistency of constraints from backreaction, which leads another condition $\xi < 6.52$ by setting $\Lambda \sim 10^{-3}M_{\mathrm{p}}$, $f \sim M_{\mathrm{p}}$, $g_* = 106.75$, and $\alpha_T^2 = 0.3$. The parameters δ_F and δ_K as a function of the e-folding number with $T/H = 25$ are plotted in Fig. 4 as well.

IV. SCALAR AND TENSOR PERTURBATION FROM THERMALIZED GAUGE FIELD

In this section, we will have detailed discussions about the spectrum of scalar perturbation, tensor perturbation, and their crossing correlation.

A. Solutions of scalar and tensor perturbation in terms of integral

The scalar perturbation related to the gauge field is obtained by varying the action with respect to ϕ,

$$\frac{1}{\sqrt{-g}}\frac{\partial}{\partial x^\nu}[\sqrt{-g}g^{\mu\nu}\partial_\mu\phi] - \frac{\mathrm{d}V}{\mathrm{d}\phi} = \frac{\alpha_c}{4f}F_{\mu\nu}\tilde{F}^{\mu\nu}. \quad (40)$$

The scalar fluctuation perturbed by the gauge field can be studied through the equation in momentum space [14]

$$\left(\frac{\partial^2}{\partial\tau^2} + k^2 - \frac{2}{\tau^2}\right)(a\delta\phi) = a^3\frac{\alpha_c}{f}\int\frac{d^3p}{(2\pi)^3}\hat{E}_i(\mathbf{k}-\mathbf{p},\tau)\hat{B}_i(\mathbf{p},\tau). \quad (41)$$

Then the equation of motion of the tensor perturbation from the Einstein equation reads

$$\left(\frac{\partial^2}{\partial\tau^2} + k^2 - \frac{2}{\tau^2}\right)(a\hat{h}_{ij}) = a^3\frac{2}{M_p^2}\Pi_{ij}{}^{mn}(\mathbf{k})\hat{T}_{mn}(\mathbf{k},\tau). \quad (42)$$

Here $\Pi_{ij,mn}(\mathbf{k}) = P_{im}(\mathbf{k})P_{jn}(\mathbf{k}) - \frac{1}{2}P_{ij}(\mathbf{k})P_{mn}(\mathbf{k})$ is the transverse traceless operator, projection operator $P_{ij}(\mathbf{k})$ is defined in Eq. (6), and $\hat{T}_{mn}(\mathbf{k})$ is the spatial component of electromagnetic energy-momentum tensor. The details of the derivation of Eqs. (41) and (42) are given in Appendix C. By decomposing tensor perturbation $\hat{h}_{ij}$ into polarized state

$$\hat{h}_{ij}(\mathbf{k},\tau) = \hat{h}_+(\mathbf{k},\tau)\mathrm{e}^+_{ij}(\mathbf{k}) + \hat{h}_-(\mathbf{k},\tau)\mathrm{e}^-_{ij}(\mathbf{k}) \quad (43)$$

and applying Eq. (B5), then Eq. (42) becomes

$$\left(\frac{\partial^2}{\partial\tau^2} + k^2 - \frac{2}{\tau^2}\right)(a\hat{h}_\lambda) = a^3\frac{2}{M_\mathrm{p}^2}\mathrm{e}^{ij}_\lambda(\mathbf{k})\cdot\int\frac{\mathrm{d}^3p}{(2\pi)^3}[\hat{E}_i(\mathbf{k}-\mathbf{p},\tau)\hat{E}_j(\mathbf{p},\tau) + \hat{B}_i(\mathbf{k}-\mathbf{p},\tau)\hat{B}_j(\mathbf{p},\tau)]. \quad (44)$$

Here, we have also used the symmetric contraction relation $g_{mn}\Pi_{ij}{}^{mn} = 0$ of the transverse traceless operator.

Equations (41) and (44) can both be solved via Green's function method:

$$a\delta\phi(\mathbf{k},\tau) = u_\mathbf{k}(\tau)\hat{b}_\mathbf{k} + u^*_\mathbf{k}(\tau)\hat{b}^\dagger_\mathbf{k} + \frac{\alpha_c}{f}\int d\eta G_k(\tau,\eta)a^3(\eta)\int\frac{\mathrm{d}^3p}{(2\pi)^3}\hat{E}_i(\mathbf{k}-\mathbf{p},\tau)\hat{B}_i(\mathbf{p},\tau), \quad (45a)$$

$$a\hat{h}_\lambda(\mathbf{k},\tau) = v_\mathbf{k}(\tau)\hat{c}_\mathbf{k} + v^*_\mathbf{k}(\tau)\hat{c}^\dagger_\mathbf{k} + \frac{2}{M_\mathrm{p}^2}\mathrm{e}^{ij}_\lambda(\mathbf{k})\int d\eta G_k(\tau,\eta)a^3(\eta)\hat{T}_{ij}(\mathbf{k},\eta), \quad (45b)$$

where $u_\mathbf{k}$ and $v_\mathbf{k}$ are scalar and tensor perturbations from vacuum fluctuation and $G_k(\tau,\eta)$ is Green's function [26,27]

$$G_k(\tau,\eta) = \frac{1}{k^3\tau\eta}[(1-k^2\tau\eta)\sin k(\tau-\eta) + k(\tau-\eta)\cos k(\tau-\eta)]\theta(\tau-\eta). \quad (46)$$

The perturbations contributed from vacuum fluctuation and the sourced thermal axionic field are statistically uncorrelated, and therefore, the total spectra can be simply obtained by the sum of them. Here, we are mainly concerned about the latter.

B. Spectrum of scalar perturbation

In the case of single field inflation, curvature perturbation $\mathcal{R} = (H/\dot{\phi})\delta\phi$ is obtained by solving Eq. (41). Then using Eq. (45a), the sourced two-point correlator of $\mathcal{R}$ corresponds to

$$\langle\hat{\mathcal{R}}(\mathbf{k},\tau)\hat{\mathcal{R}}(\mathbf{k}',\tau)\rangle = \frac{H^2}{\dot{\phi}^2}\frac{\alpha_c^2}{a^2f^2}\int d\eta_1 G_k(\tau,\eta_1)a(\eta_1)^3\cdot\int d\eta_2 G_{k'}(\tau,\eta_2)a(\eta_2)^3\int\frac{d^3p}{(2\pi)^3}\frac{d^3q}{(2\pi)^3} \cdot\langle\hat{E}_i(\mathbf{k}-\mathbf{p},\eta_1)\hat{B}_i(\mathbf{p},\eta_2)\hat{E}_j(\mathbf{k}'-\mathbf{q}\eta_2)\hat{B}_j(\mathbf{q},\eta_2)\rangle. \quad (47)$$

The ensemble average on the right-hand side of the equation contains four field operators, and it can be decomposed into three terms with two ensemble averages of each due to the Wick theorem [28]:

$$\left\langle\hat{E}_i(\mathbf{k}-\mathbf{p},\eta_1)\hat{B}_i(\mathbf{p},\eta_1)\hat{E}_j(\mathbf{k}'-\mathbf{q},\eta_2)\hat{B}_j(\mathbf{q},\eta_2)\right\rangle = \left\langle\hat{E}_i(\mathbf{k}-\mathbf{p},\eta_1)\hat{B}_i(\mathbf{p},\eta_1)\right\rangle\left\langle\hat{E}_j(\mathbf{k}'-\mathbf{q},\eta_2)\hat{B}_j(\mathbf{q},\eta_2)\right\rangle + \left\langle\hat{E}_i(\mathbf{k}-\mathbf{p},\eta_1)\hat{E}_j(\mathbf{k}'-\mathbf{p},\eta_2)\right\rangle\left\langle\hat{B}_i(\mathbf{p},\eta_1)\hat{B}_j(\mathbf{q},\eta_2)\right\rangle + \left\langle\hat{E}_i(\mathbf{k}-\mathbf{p},\eta_1)\hat{B}_j(\mathbf{q},\eta_2)\right\rangle\left\langle\hat{B}_i(\mathbf{p},\eta_1)\hat{E}_j(\mathbf{k}'-\mathbf{q},\eta_2)\right\rangle. \quad (48)$$

Equation (48) contains an unequal time correlation of two fields. At equilibrium, a two-time correlation function decays exponentially as a function of dissipative coefficient [27]: $\langle X_i(\mathbf{p},\eta_1)X_j'(\mathbf{q},\eta_2)\rangle = \langle X_i(\mathbf{p},\eta)X_j'(\mathbf{q},\eta)\rangle e^{-\Gamma_A|t_1-t_2|}$, where $\eta = \min(\eta_1,\eta_2)$ and Γ_A is the dissipative coefficient of the gauge field. Generally, Γ_A relates to quantum effects, such as the Schwinger effect [29], and we assume the freeze-out scale of the Schwinger effect is larger than any observable cosmic scale k, i.e., $\Gamma_A \ll k$. In fact, the value of Γ_A does not generate significant observational effects, as mathematically shown in Eq. (D8). On the other hand, the first term on the right-hand side of Eq. (48) contains only the disconnected diagram proportional to $\delta(\mathbf{k})\delta(\mathbf{k}')$, and this term could be ignored. Considering the symmetry of η_1 and η_2 and the superhorizon limit $k \to 0$, then the correlation function (47) corresponds to

$$\begin{aligned}\langle\hat{\mathcal{R}}(\mathbf{k},\tau)\hat{\mathcal{R}}(\mathbf{k}',\tau)\rangle = {} & 2\frac{H^2}{\dot\phi^2}\frac{\alpha_c^2H^2}{f^2}\frac{1}{k^2k'^2}\int_{-\infty}^{0}d\eta_1\frac{\sin k\eta_1 - k\eta_1\cos k\eta_1}{k\eta_1}a^3(\eta_1)\int_{-\infty}^{\eta_1}d\eta_2\frac{\sin k'\eta_2 - k'\eta_2\cos k'\eta_2}{k'\eta_2}a^3(\eta_2)\\ & \cdot e^{-2\Gamma_A|\eta_1-\eta_2|}\int\frac{d^3p}{(2\pi)^3}\int\frac{d^3q}{(2\pi)^3}\cdot 2(2\pi)^6\delta^3(\mathbf{k}+\mathbf{k}')\delta^3(\mathbf{p}+\mathbf{q})a^{-4}(\eta_1)a^{-4}(\eta_2)\eta_2^2p^4\\ & \cdot\{n_B(\omega_{|\mathbf{k}-\mathbf{p}|}/aT)n_B(\omega_p/aT)[P_B(p,\eta_2)P_E(p,\eta_2)+S_B(p,\eta_2)S_E(p,\eta_2)]\\ & + n_B^2(\omega_p/aT)[P_c^2(p,\eta_2)+S_c^2(p,\eta_2)]\}.\end{aligned} \tag{49}$$

Here we have set $\eta_2 < \eta_1$ and the factor of 2 in front of the right-hand side comes from its opposite situation $\eta_2 > \eta_1$. Notice that the integral over $\mathbf{p}$ of $n_B(\omega_{|\mathbf{k}-\mathbf{p}|}/aT)$ diverges as long as $k > 0$, and then the thermal mass should be taken into account in the Bose-Einstein distribution function as shown in Eq. (23). The details on computation of the scalar correlator have been shown in Appendix D, and we give only the final approximate results here:

$$\begin{aligned}\langle\mathcal{R}(\mathbf{k},\tau)\mathcal{R}(\mathbf{k}',\tau)\rangle \approx {} & 2\pi\left(\frac{H^2}{\dot\phi}\right)^2\left(\frac{\alpha_cM_p}{f}\right)^2\left(\frac{H}{M_p}\right)^2\frac{1}{k^3}\delta^3(\mathbf{k}+\mathbf{k}')\cdot\left(\frac{\pi}{3}+\frac{2}{3}(5-8\ln 2)\frac{\Gamma}{k}\right)\\ & \times\left|\frac{(1+\ell)\Gamma^2(2\ell+2)}{(2\ell+1)^2\cdot 2^{2\ell}}\right|^2\left(\frac{e^{2\pi\xi}}{|\Gamma(\ell+1+i\xi)|^4}+\frac{e^{-2\pi\xi}}{|\Gamma(\ell+1-i\xi)|^4}\right)\\ & \times\begin{cases}\left(\frac{T}{H}\right)^{5-4\ell}\Gamma(5-4\ell)\left[2\sum_{n=1}^{\infty}\zeta(5-4\ell,n+1)e^{-n\alpha_T}+2\zeta(5-4\ell)-2\right], & 4\mu^2<1\\ \left(\frac{T}{H}\right)^7\Gamma(7)e^{-\sqrt{4\mu^2-1}/2}\left[2\frac{e^{\alpha_T}\mathrm{Li}_7(e^{-\alpha_T})-\zeta(7)}{e^{\alpha_T}-1}+2\zeta(7)-2\right], & 4\mu^2<1\end{cases}\\ \approx {} & \frac{4\pi^2}{3}\left(\frac{H^2}{\dot\phi}\right)^2\left(\frac{\alpha_cM_p}{f}\right)^2\left(\frac{H}{M_p}\right)^2\frac{1}{k^3}\delta^3(\mathbf{k}+\mathbf{k}')\left|\frac{(1+\ell)\Gamma^2(2\ell+2)}{(2\ell+1)^2\cdot 2^{2\ell}}\right|^2\left(\frac{e^{2\pi\xi}}{|\Gamma(\ell+1+i\xi)|^4}+\frac{e^{-2\pi\xi}}{|\Gamma(\ell+1-i\xi)|^4}\right)\\ & \times\begin{cases}\left(\frac{T}{H}\right)^{5-4\ell}\Gamma(5-4\ell)[2^{-(5-4\ell)}e^{-\alpha_T}+\zeta(5-4\ell)-1], & 4\mu^2<1\\ \left(\frac{T}{H}\right)^7\Gamma(7)[2^{-7}e^{-\alpha_T}+\zeta(7)-1], & 4\mu^2>1\end{cases}\end{aligned} \tag{50}$$

with μ^2 defined in Eq. (13).

It is still not convenient to obtain the numerical results from Eq. (50) if $\mu \gg 1$ or $T/H \gg 1$. The limit $T/H \gg 1$ leads the approximations $\ell \approx -1/2 + i\mu$ with $\mu \gg 1$. The asymptotic form of Gamma function [24] $|\Gamma(x+iy)| \simeq \sqrt{2\pi}|y|^{x-(1/2)}e^{-\pi|y|/2}$ (as $|y| \gg 1$) helps to simplify the expression

$$|\Gamma(2\ell+2)|^4\left(\frac{e^{2\pi\xi}}{|\Gamma(\ell+1+i\xi)|^4}+\frac{e^{-2\pi\xi}}{|\Gamma(\ell+1-i\xi)|^4}\right) \approx 16\mu^2(e^{4\pi\xi}+1). \tag{51}$$

Because of the definition (18), the thermal sourced spectral density function of scalar perturbation from Eq. (50) could be simplified as

$$\mathcal{P}_{\mathcal{R}}^{(s)} \approx \frac{2}{3}\left(\frac{T}{H}\right)^7\left(\frac{\xi}{\varepsilon}\right)^2\left(\frac{H}{M_p}\right)^4\frac{1}{|2^\ell|^4}(e^{4\pi\xi}+1)\Gamma(7)[2^{-7}e^{-\alpha_T}+\zeta(7)-1]. \tag{52}$$

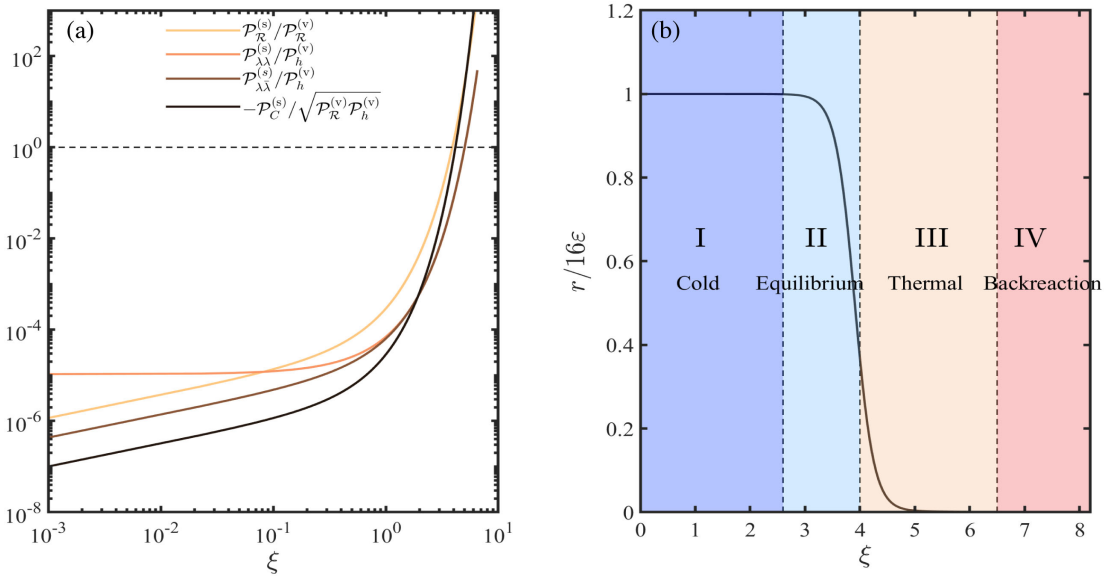

FIG. 5. (a) Curves of ratios $\mathcal{P}_{\mathcal{R}}^{(s)}/\mathcal{P}_{\mathcal{R}}^{(v)}$, $\mathcal{P}_{\lambda\lambda}^{(s)}/\mathcal{P}_{h}^{(v)}$, $\mathcal{P}_{\lambda\bar{\lambda}}^{(s)}/\mathcal{P}_{h}^{(v)}$, and $-\mathcal{P}_{C}^{(s)}/\sqrt{\mathcal{P}_{\mathcal{R}}^{(v)}\mathcal{P}_{h}^{(v)}}$ to ξ by setting $\Lambda = 10^{-3}M_{\rm p}$, $f = M_{\rm p}$, $\varepsilon = 0.01$, and $\alpha_T^2 = 0.3$. (b) Curve of tensor-to-scalar ratio $r/16\varepsilon$ with the same parameter combination. The areas I–IV from left to right are cold regime, equilibrium regime, thermal regime, and backreaction regime, respectively.

Figure 5(a) plots the ratio of the thermal sourced scalar density spectrum to vacuum spectrum $\mathcal{P}_{\mathcal{R}}^{(s)}/\mathcal{P}_{\mathcal{R}}^{(v)}$, where $\mathcal{P}_{\mathcal{R}}^{(v)} = \frac{H^2}{8\pi^2\epsilon_\phi M_{\rm p}^2}$ is the scalar density spectrum from the vacuum. The intersection point of the curve and horizontal unit line locates at $\xi \approx 4.0$, or $T/H \approx 105$, by setting $\Lambda = 10^{-3}M_{\rm p}$, $f = M_{\rm p}$, $\varepsilon = 0.01$, and $\alpha_T^2 = 0.3$. The thermalized condition is almost the same as the result in Ref. [15], meaning the thermalization of axionic inflation happens.

C. Spectrum of tensor perturbation

The correlation function of tensor perturbation contains two parts: correlation of the same polarization state and the opposite polarization state. From Eq. (44), the tensor perturbation correlator of polarization state λ and λ' reads

$$\begin{aligned}\left\langle \hat{h}_\lambda(\mathbf{k},\tau)\hat{h}_{\lambda'}(\mathbf{k}',\tau)\right\rangle = {}& \frac{4}{M_p^4 a^2}\int {\rm d}\eta_1 G_k(\tau,\eta_1)a^3(\eta_1)\int {\rm d}\eta_2 G_{k'}(\tau,\eta_2)a^3(\eta_2)\\ & \times e_\lambda^{ij}(\mathbf{k})e_{\lambda'}^{mn*}(\mathbf{k})\int\frac{{\rm d}^3p}{(2\pi)^3}\int\frac{{\rm d}^3q}{(2\pi)^3}\Big[\left\langle \hat{B}_i(\mathbf{k}-\mathbf{p},\eta_1)\hat{B}_j(\mathbf{p},\eta_1)\hat{B}_m(\mathbf{k}-\mathbf{p},\eta_2)\hat{B}_n(\mathbf{p},\eta_2)\right\rangle\\ & +2\left\langle \hat{B}_i(\mathbf{k}-\mathbf{p},\eta_1)\hat{B}_j(\mathbf{p},\eta_1)\hat{E}_m(\mathbf{k}-\mathbf{p},\eta_2)\hat{E}_n(\mathbf{p},\eta_2)\right\rangle + \left\langle \hat{E}_i\hat{E}_j\hat{E}_m\hat{E}_n\right\rangle\Big].\end{aligned} \tag{53}$$

Here we only show the computations containing four magnetic field operators as an example. Applying a similar approximation in Appendix D, the contraction in Eq. (53) becomes

$$\begin{aligned}& e_\lambda^{ij}(\mathbf{k})e_{\lambda'}^{mn*}(\mathbf{k})\left\langle \hat{B}_i(\mathbf{k}-\mathbf{p},\eta_1)\hat{B}_j(\mathbf{p},\eta_1)\hat{B}_m(\mathbf{k}-\mathbf{p},\eta_2)\hat{B}_n(\mathbf{p},\eta_2)\right\rangle\\ & \quad\propto \epsilon_\lambda^i(\mathbf{k})\epsilon_\lambda^j(\mathbf{k})\epsilon_\lambda^{m*}(\mathbf{k})\epsilon_\lambda^{n*}(\mathbf{k})\left\{n_{\rm B}(\omega_{|\mathbf{k}-\mathbf{p}|}/aT)n_{\rm B}(\omega_p/aT)\left[(\delta_{im}-\hat{p}_i\hat{p}_m)P_B(p,\eta)+{\rm i}\eta_{iml}\hat{p}^l S_B(p,\eta)\right]\right.\\ & \quad\left.+n_{\rm B}^2(\omega_p/aT)\left[(\delta_{jn}-\hat{p}_j\hat{p}_n)P_B(p,\eta)+{\rm i}\eta_{jnl}\hat{p}^l S_B(p,\eta)\right]\right\}\\ & \quad= \left[n_B^2(\omega_p/aT)+n_{\rm B}(\omega_{|\mathbf{k}-\mathbf{p}|}/aT)n_{\rm B}(\omega_p/aT)\right]\left[\left(\delta_{\lambda\lambda'}-\frac{1}{2}\sin^2\theta{\rm e}^{{\rm i}(\lambda-\lambda')\varphi}\right)^2 P_B^2(p,\eta)+\cos^2\theta(1-\delta_{\lambda\lambda'})S_B^2(p,\eta)\right],\end{aligned} \tag{54}$$

with $\eta = \min(\eta_1,\eta_2)$. In the last step, Eqs. (B8)–(B13) have been applied. Note that if $\lambda = \lambda'$, the term $\cos^2\theta(1-\delta_{\lambda\lambda'})$ in the last step vanishes, and if $\lambda \neq \lambda'$ (or $\lambda = \bar{\lambda}'$), the term $\sin^2\theta{\rm e}^{{\rm i}(\lambda-\lambda')\varphi}$ vanishes after integrating over φ since $\int_0^{2\pi}{\rm d}\varphi{\rm e}^{\pm{\rm i}2\varphi} = 0$. So Eq. (54) contains the important information about polarization correlation.

With the help of the discussions above and taking the remaining two terms on the right-hand side of (53), it yields the correlator of tensor perturbation with the same polarization mode

$$\left\langle \hat{h}_\lambda(\mathbf{k},\tau)\hat{h}_\lambda(\mathbf{k}',\tau)\right\rangle = \frac{8\pi^2}{5}\frac{H^4}{M_p^4}\frac{1}{k^3}\delta^3(\mathbf{k}+\mathbf{k}')\left|\frac{(2-\ell)\Gamma^2(2\ell+2)}{(2\ell+1)^2\cdot 2^{2\ell}}\right|^2\left(\frac{e^{\pi\xi}}{|\Gamma(\ell+1+i\xi)|^2}+\frac{e^{-\pi\xi}}{|\Gamma(\ell+1-i\xi)|^2}\right)^2 \times\begin{cases}\left(\frac{T}{H}\right)^{4-4\ell}\Gamma(4-4\ell)[2^{-(4-4\ell)}e^{-\alpha_T}+\zeta(4-4\ell)-1], & 4\mu^2<1\\ \left(\frac{T}{H}\right)^6\Gamma(6)[2^{-6}e^{-\alpha_T}+\zeta(6)-1], & 4\mu^2>1\end{cases} \tag{55}$$

and the opposite polarization mode

$$\left\langle \hat{h}_\lambda(\mathbf{k},\tau)\hat{h}_{\bar{\lambda}}(\mathbf{k}',\tau)\right\rangle = \frac{16\pi^2}{9}\frac{H^4}{M_p^4}\frac{1}{k^3}\delta^3(\mathbf{k}+\mathbf{k}')\left|\frac{(2-\ell)\Gamma^2(2\ell+2)}{(2\ell+1)^2\cdot 2^{2\ell}}\right|^2\left(\frac{e^{\pi\xi}}{|\Gamma(\ell+1+i\xi)|^2}-\frac{e^{-\pi\xi}}{|\Gamma(\ell+1-i\xi)|^2}\right)^2 \times\begin{cases}\left(\frac{T}{H}\right)^{4-4\ell}\Gamma(4-4\ell)[2^{-(4-4\ell)}e^{-\alpha_T}+\zeta(4-4\ell)-1], & 4\mu^2<1\\ \left(\frac{T}{H}\right)^6\Gamma(6)[2^{-6}e^{-\alpha_T}+\zeta(6)-1]. & 4\mu^2>1\end{cases} \tag{56}$$

Repeating the asymptotic analysis in Sec. IV B, we have the approximate spectral density of tensor perturbation with the same and the opposite polarization modes

$$\mathcal{P}^{(s)}_{\lambda\lambda}\approx\frac{4}{5}\left(\frac{T}{H}\right)^6\left(\frac{H}{M_p}\right)^4\frac{1}{|2^\ell|^4}(e^{2\pi\xi}+1)^2\Gamma(6)[2^{-6}e^{-\alpha_T}+\zeta(6)-1] \tag{57}$$

and

$$\mathcal{P}^{(s)}_{\lambda\bar{\lambda}}\approx\frac{8}{3}\left(\frac{T}{H}\right)^6\left(\frac{H}{M_p}\right)^4\frac{1}{|2^\ell|^4}(e^{2\pi\xi}-1)^2\Gamma(6)[2^{-6}e^{-\alpha_T}+\zeta(6)-1]. \tag{58}$$

Figure 5(a) plots the curves of ratios $\mathcal{P}^{(s)}_{\lambda\lambda}/\mathcal{P}^{(v)}_h$ and $\mathcal{P}^{(s)}_{\lambda\bar{\lambda}}/\mathcal{P}^{(v)}_h$, where $\mathcal{P}^{(v)}_h=\frac{2H^2}{\pi^2M_p^2}$ is the spectral density of vacuum tensor perturbation. It is clear from the figure or from Eq. (56) that $\mathcal{P}^{(s)}_{\lambda\bar{\lambda}}=0$ if $\xi=0$. The critical value ξ or T/H to thermalize the geometrical tensor perturbation is slightly larger than that of scalar perturbation, and we still use $\xi=4.0$ as the critical value of thermalization.

D. Spectrum of crossing correlation between scalar and tensor perturbations

The correlator between scalar and tensor perturbations reads

$$\begin{aligned}\langle\hat{\mathcal{R}}(\mathbf{k},\tau)\hat{h}_\lambda(\mathbf{k}',\tau)\rangle = {}& \frac{2}{M_p^2}\frac{H}{\dot{\phi}}\frac{\alpha_c}{f}\frac{1}{a^2}\int d\eta_1 G_k(\tau,\eta_1)a^3(\eta_1)\\ &\times\int d\eta_2 G_k(\tau,\eta_2)a^3(\eta_2)e^{mn}_\lambda(\mathbf{k})\int\frac{d^3p}{(2\pi)^3}\int\frac{d^3p}{(2\pi)^3}\left\langle\hat{E}_i(\mathbf{p},\eta_1)\hat{B}_i(\mathbf{k}-\mathbf{p},\eta_1)\right.\\ &\times\left.\left[\hat{B}_m(\mathbf{q},\eta_2)\hat{B}_n(\mathbf{k}'-\mathbf{q},\eta_2)+\hat{E}_m(\mathbf{q},\eta_2)\hat{E}_n(\mathbf{k}'-\mathbf{q},\eta_2)\right]\right\rangle.\end{aligned} \tag{59}$$

The part with the contraction becomes

$$\begin{aligned}&e^{mn}_\lambda(\mathbf{k})\int d^3p\int d^3q[\left\langle\hat{E}_i(\mathbf{p})\hat{B}_m(\mathbf{q})\right\rangle\left\langle\hat{B}_i(\mathbf{k}-\mathbf{p})\hat{B}_n(\mathbf{k}'-\mathbf{q})\right\rangle+\left\langle\hat{E}_i(\mathbf{p})\hat{B}_n(\mathbf{k}-\mathbf{q})\right\rangle\left\langle\hat{B}_i(\mathbf{k}-\mathbf{p})\hat{B}_n(\mathbf{q})\right\rangle]\\ &\propto\int d^3p e^{mn}_\lambda(\mathbf{k})[-(\delta_{im}-\hat{p}_i\hat{p}_m)S_C(p)+i\eta_{iml}\hat{p}^l P_C(p)]\\ &\cdot[(\delta_{in}-\hat{p}_i\hat{p}_n)P_B(p)+i\eta_{inl}\hat{p}^l S_B(p)][n_B^2(\omega_p/aT)+n_B(\omega_p/aT)n_B(\omega_{|\mathbf{k}-\mathbf{p}|}/aT)]\end{aligned}$$

$$= \int \mathrm{d}^3p \left[\frac{1}{2}\sin^2\theta \mathrm{e}^{\mathrm{i}\lambda\varphi}(S_C P_B + P_C S_B)(p) + \cos\theta(S_C S_B + P_C P_B)(p)\right][n_{\mathrm{B}}^2(\omega_p/aT) + n_{\mathrm{B}}(\omega_p/aT)n_{\mathrm{B}}(\omega_{|\mathbf{k}-\mathbf{p}|}/aT)]$$
$$= \int \mathrm{d}^3p \cos\theta[S_C S_B + P_C P_B](p) n_{\mathrm{B}}(\omega_p/aT) n_{\mathrm{B}}(\omega_{|\mathbf{k}-\mathbf{p}|}/aT). \tag{60}$$

In the second step of the equation above, Eqs. (B12) and (B13) have been used, and, in the third step, integrals $\int_0^{2\pi} \mathrm{d}\varphi \mathrm{e}^{\mathrm{i}\lambda\varphi} = \int_0^{\pi} \mathrm{d}\theta \sin\theta\cos\theta = 0$ have been used. Then the correlation function (59) is written as

$$\begin{aligned}\left\langle \hat{\mathcal{R}}(\mathbf{k},\tau)\hat{h}_\lambda(\mathbf{k}',\tau)\right\rangle &= \frac{2\pi^2}{3}\frac{H^3}{M_p^3}\frac{H^2}{\dot\phi}\frac{\alpha_c M_p}{f}\frac{1}{k^3}\delta^3(\mathbf{k}+\mathbf{k}')\int \mathrm{d}x x^6 (S_C S_B - S_C S_E + P_C P_B - P_C P_E)(x) \\ &\cdot \sum_{m=1}^{\infty} -\frac{\mu^2}{3x}\mathrm{e}^{-m(H/T)x}\mathrm{e}^{-m(H/T)(\sqrt{\mu^2+\tilde{k}_p^2}-\tilde{k}_p)}\sum_{n=1}^{\infty}\mathrm{e}^{-n(H/T)x} \\ &\approx \frac{4\pi^2}{9}\left(\alpha_T\frac{T}{H}\right)^2\frac{H^3}{M_p^3}\frac{H^2}{\dot\phi}\frac{\alpha_c M_p}{f}\frac{1}{k^3}\delta^3(\mathbf{k}+\mathbf{k}')\cdot\frac{|\ell(1-\ell)(2-\ell)|}{|\Gamma(\ell+1+\mathrm{i}\xi)\Gamma(\ell+1-\mathrm{i}\xi)|^2}\cdot\left|\frac{\Gamma(2\ell+2)}{(2\ell+2)\cdot 2^\ell}\right|^4 \\ &\cdot\begin{cases}\left(\frac{T}{H}\right)^{4-4\ell}\Gamma(4-4\ell)[2^{-(4-4\ell)}\mathrm{e}^{-\alpha_T}+\zeta(4-4\ell)-1], & 4\mu^2<1\\ \left(\frac{T}{H}\right)^6\Gamma(6)[2^{-6}\mathrm{e}^{-\alpha_T}+\zeta(6)-1]. & 4\mu^2>1\end{cases}.\end{aligned} \tag{61}$$

Express the spectral density of the scalar-tensor crossing at limit $T/H \gg 1$ approximately

$$\mathcal{P}_C^{(\mathrm{s})} \approx -\frac{2}{9}\left(\frac{T}{H}\right)^8\frac{\alpha_T\xi}{\varepsilon}\left(\frac{H}{M_p}\right)^4\Gamma(6)[2^{-6}\mathrm{e}^{-\alpha_T}+\zeta(6)-1]. \tag{62}$$

It is also obvious that the crossing correlation comes from the one-loop renormalization coefficient α_T or thermal mass. Figure 5(a) also plots the curves of ratio $-\mathcal{P}_C^{(\mathrm{s})}/\sqrt{\mathcal{P}_{\mathcal{R}}^{(\mathrm{v})}\mathcal{P}_h^{(\mathrm{v})}}$.

E. Numerical results of tensor-to-scalar ratio

Because of the equation mentioned in Eq. (45), the perturbations consist of two parts: vacuum and sourced from the thermal gauge field. The vacuum part is expressed as the standard form

$$\mathcal{P}_{\mathcal{R}}^{(v)}(k) = \frac{H^2}{8\pi^2\varepsilon M_{\mathrm{p}}^2}, \qquad \mathcal{P}_{\pm}^{(v)}(k) = \frac{H^2}{\pi^2 M_{\mathrm{p}}^2}, \tag{63}$$

where $\varepsilon = \dot\phi^2/(2H^2M_{\mathrm{p}}^2)$ is the slow-roll parameter controlled by the axionic inflaton. The sourced spectral density $\mathcal{P}_{\mathcal{R}}^{(s)}(k)$ and $\mathcal{P}_{\pm}^{(s)}(k)$ are obtained from Eqs. (50) and (55). The quantum and thermal parts are statistically uncorrelated, so the total spectrum could be simply described by the sum of them. Then the tensor-to-scalar ratio contributed from the vacuum and sourced parts reads

$$r = \sum_{\lambda=\pm}\frac{\mathcal{P}_\lambda^{(\mathrm{v})}(k)+\mathcal{P}_{\lambda\lambda}^{(\mathrm{s})}(k)}{\mathcal{P}_{\mathcal{R}}^{(\mathrm{v})}(k)+\mathcal{P}_{\mathcal{R}}^{(\mathrm{s})}(k)} = 16\varepsilon\left[\frac{1+\sum_\lambda\frac{1}{16\varepsilon}\mathcal{P}_{\lambda\lambda}^{(\mathrm{s})}(k)/\mathcal{P}_{\mathcal{R}}^{(\mathrm{v})}(k)}{1+\mathcal{P}_{\mathcal{R}}^{(\mathrm{s})}(k)/\mathcal{P}_{\mathcal{R}}^{(\mathrm{v})}(k)}\right]. \tag{64}$$

In Fig. 5(b), we show the line of tensor-to-scalar ratio r corrected by thermal effects as a function of ξ. It is seen that the ratio $r/16\varepsilon$ tends toward 1 if $\xi < 3.0$, which indicates that no thermalization has occurred, and the ratio drops dramatically when $\xi > 3.0$. At the threshold of thermalization $\xi = 4.0$, the ratio $r/16\varepsilon$ falls to nearly $1/\mathrm{e}$. Four regions mentioned in this paper are labeled I–IV from left to right in the figure. Tensor-to-scalar ratio r is mathematically suppressed by

$$r \approx \frac{5.12}{\xi^2}\frac{H}{T} \sim 0.3H/T, \qquad \xi \gtrsim 4.0. \tag{65}$$

Reference [15] has shown that r is suppressed by $H/2T$ when thermalization of axion fields happens. In addition, Eq. (65) is also a typical result for warm inflation in the weak dissipation regime [30,31]. The slight difference may come from the difference of the approximation method. Another interesting phenomenon is that when $\xi < 3.0$, the tensor-to-scalar ratio $r \simeq 16\varepsilon$ is the same as that in cold inflation, although thermal effects are taken into consideration. This indicates that only when the value of ξ is large enough or the cosmic temperature T is high enough will it have a significant impact on the cosmic perturbation, so the

cold axion inflation is still a reasonable model from this respective when $\xi < 3.0$.

V. CONCLUSIONS AND FURTHER DISCUSSIONS

In this paper, we investigate a model of axion inflaton interacting with the U(1) gauge field through the Chern-Simons term. Two thermal effects have been introduced: ensemble average and thermal mass. The former leads to a Bose-Einstein distribution of the gauge field and eliminates the divergence at a short wavelength. The latter makes the gauge field obtain an additional mass in the equation of motion via one-loop correction. Larger α_T can reduce the cosmic temperature T due to a suppression on the thermal effect. Theoretical and numerical calculations confirm that cosmic temperature T and Hubble parameter H always appear in the form of a ratio T/H, meaning a competition between the thermal effect and the geometric effect. The constraints from the thermal equilibrium condition and backreaction predict a parametric range of $2.47 < \xi < 6.52$. In addition, we also confirm that the threshold of field thermalization is $\xi \approx 4.0$. Another important conclusion is that the adiabatic approximation always corresponds to a slow-roll approximation, which may indicate that cosmic temperature tends to a constant during the inflationary epoch. At last, Green's function method is applied to calculate the thermal sourced spectral density of scalar and tensor perturbation by assuming adiabatic temperature changes. Analytical expressions show that a larger value of the parameter ξ enhances the cosmic thermal effects and increases the sourced spectral density of scalar perturbation and tensor perturbation. In addition, a new effect from thermal mass is the appearance of the crossing correlation of scalar perturbation and tensor perturbation, which may be a potential method to distinguish inflationary models. Theoretical calculations together with numerical analysis show that the tensor-to-scalar ratio r is suppressed by approximately $0.3H/T$ if the axion is thermalized, but if $\xi < 3.0$, the model is consistent with the cold inflation model even if the gauge field is already thermal.

Let us now discuss the similarities and differences between the present model involved and the warm inflationary model [1,2,30–34], which may offer a better understanding on thermal effects of the early universe. The similarities between the two scenarios can be summarized as follows:

(i) They both predict an equilibrium thermal bath with $T/H > 1$ and the energy density of radiation to satisfy the condition $\rho_r \ll V$.
(ii) Both cosmic temperatures tend to a constant during the inflation era, which means a holding on adiabatic approximation.
(iii) They both show an enhancement on scalar perturbation from thermal effects with respect to cold inflation, leading to a suppressed tensor-to-scalar ratio.
(iv) Similar to the conclusions in this work, the cosmic temperature in warm axion inflation is still controlled by the coupling strength α_C, despite the specific relationship depending on α_C being different [16].
(v) The final result for the tensor-to-scalar ratio in Eq. (65) is also typical of warm inflation in the weak dissipation regime [30,31]. This is a clear indication that the model can be an explicit warm inflation realization. This indicates an intimate relation between the scenarios of cold inflation and warm inflation when a thermal bath is taken into account, though more study in understanding this connection is worth being carried out in the future. Additionally, the generation of a thermal radiation bath during inflation may also claim that it provides a realization of warm inflation starting from a vacuum state.

The similarities discussed above can be summarized as follows: in the two research schemes, there is almost no difference in thermodynamic properties, and temperature has an impact on cosmological observations in the same form. From this perspective, it is reasonable to study the thermodynamic effects of the very early universe based on the fundamental principles of thermodynamics.

The differences can be summarized as follows:

(i) Mechanisms for generating the thermal bath are different. Warm inflation suggests that the thermal bath is produced via thermal damping, which is described by a dissipation term coupling to the velocity of inflaton, while, in this paper, the thermal bath is from the scattering between the axion and gauge fields, which is described by a Boltzmann equation [15]. But, a similarity could be found that the generation rates of the thermal background in two models are both dependent on the velocity of the inflation field.
(ii) Perturbations are generated from different mechanisms. In warm inflation, the field perturbations originate directly from the thermal bath which is driven by a thermal fluctuation. But, in this work, we still take the quantum fluctuation into consideration and regard the gauge fields as a sourced thermal fluctuation.
(iii) Warm inflation predicts a direct decrease of temperature without reheating, but we do not summarize any similar or opposite conclusions in this paper, which needs further study on this problem.

Although there are still some inconsistencies or issues that need to be clarified, the above similarities are enough to help us understand the thermal effect: this effect may be an unavoidable cosmological phenomenon in the early universe and may compact on the observational parameters, such as the tensor-to-scalar ratio. To better and further understand this phenomenon, it is worth introducing new

models, which is also what we are preparing to do in the next work.

ACKNOWLEDGMENTS

The authors are grateful to Professor Dr. Francois Guillou for comments on a draft of this paper. We also express our gratitude to the reviewer for the enlightening comments. This work was supported by the National Natural Science Foundation of China (Grant No. 11864030), Inner Mongolia Natural Science Foundation (Grant No. 2021LHBS01001), and Scientific Research Funding Project for Introduced High Level Talents of IMNU (Grant No. 2020YJRC001).

APPENDIX A: COULOMB FUNCTION WITH COMPLEX PARAMETERS

The Coulomb function is obtained by solving the ordinary differential equation

$$\frac{\mathrm{d}^2\psi}{\mathrm{d}\rho^2}+\left(1-\frac{2\eta}{\rho}-\frac{\ell(\ell+1)}{\rho^2}\right)\psi=0. \tag{A1}$$

This equation often appears in the model of a hydrogen atom in terms of the Schrödinger equation, in which the parameter ℓ is required to be a non-negative integer as $\ell=0,1,2,\ldots$. But here, parameter ℓ is a complex number with $\mathrm{Re}\ell\geq -1/2$, and related properties are cited from Ref. [35]. The two linearly independent solutions of Eq. (A1) are Coulomb functions $F_\ell(\eta,\rho)$ and $G_\ell(\eta,\rho)$ or $H_\ell^{\pm}(\eta,\rho)=G_\ell(\eta,\rho)\pm \mathrm{i}F_\ell(\eta,\rho)$, with asymptotic relation

$$H_\ell^{\pm}(\eta,\rho)\sim \exp\{\pm\mathrm{i}[\rho-\eta\ln(2\rho)-\ell\pi/2+\sigma_\ell(\eta)]\}\cdot\sum_{k=0}^{\infty}\binom{L+\mathrm{i}\eta}{k}\left(\frac{\pm 1}{2\mathrm{i}\rho}\right)^k\frac{\Gamma(-\ell\mp\mathrm{i}\eta)}{\Gamma(-\ell\mp\mathrm{i}\eta-k)},\quad |\rho|\gg 1. \tag{A2}$$

Phase $\sigma_\ell(\eta)$ is defined as

$$\sigma_\ell(\eta)=\frac{1}{2\mathrm{i}}[\ln\Gamma(\ell+1+\mathrm{i}\eta)-\ln\Gamma(\ell+1-\mathrm{i}\eta)] \tag{A3}$$

or

$$\mathrm{e}^{-\mathrm{i}\sigma_\ell(\eta)}=\left(\frac{\Gamma(\ell+1-\mathrm{i}\eta)}{\Gamma(\ell+1+\mathrm{i}\eta)}\right)^{1/2}, \tag{A4}$$

where $\Gamma(z)$ is the Gamma function. Notice that the phase $\sigma_\ell(\eta)$ is always a real number when η is real. The limit form of the Coulomb functions reads

$$F_\ell(\eta,\rho)=\frac{[\Gamma(\ell+1+\mathrm{i}\eta)\Gamma(\ell+1-\mathrm{i}\eta)]^{\frac{1}{2}}}{2\exp(\eta\pi/2)\Gamma(2\ell+2)}(2\rho)^{\ell+1}\cdot\sum_{k=0}^{\infty}D_{\ell,k}(\eta)\rho^k\approx C_\ell(\eta)\rho^{\ell+1} \tag{A5}$$

and

$$G_\ell(\eta,\rho)\approx\frac{\rho^{-\ell}}{(2\ell+1)C_\ell(\eta)},\quad \text{as } |\rho|\to 0, \tag{A6}$$

where the Gamow factor writes

$$C_\ell(\eta)=\frac{2^\ell \mathrm{e}^{-\pi\eta/2}[\Gamma(\ell+1+\mathrm{i}\eta)\Gamma(\ell+1-\mathrm{i}\eta)]^{\frac{1}{2}}}{\Gamma(2\ell+2)}. \tag{A7}$$

A special case of $\ell=-1/2$ approximates

$$F_{-1/2}(\eta,\rho)=\left(\frac{\pi}{\exp(2\pi\eta)+1}\right)^{1/2}\rho^{1/2}\sum_{k=0}^{\infty}c_{-1/2,k}\rho^k,\quad c_{-1/2,0}=1, \tag{A8}$$

and

$$\frac{G_{-1/2}(\eta,\rho)}{F_{-1/2}(\eta,\rho)}=\frac{\exp(2\pi\eta)+1}{\pi}[\ln(1/\rho)+4\eta\rho+\cdots]. \tag{A9}$$

Coulomb functions also relate to Whittaker equation

$$H_\ell^{\pm}(\eta,\rho)=(\mp\mathrm{i})^\ell \mathrm{e}^{\pi\eta/2\pm\mathrm{i}\sigma_\ell(\eta)}W_{\mp\mathrm{i}\eta,\ell+\frac{1}{2}}(\mp 2i\rho). \tag{A10}$$

APPENDIX B: VECTORS AND TENSORS

The transverse-traceless projector is defined as

$$\Pi_{ij,mn}(\mathbf{k})=P_{im}(\mathbf{k})P_{jn}(\mathbf{k})-\frac{1}{2}P_{ij}(\mathbf{k})P_{mn}(\mathbf{k}), \tag{B1}$$

where $P_{ij}(\mathbf{k})=\delta_{ij}-\hat{k}_i\hat{k}_j$ is the transverse projection operator with unit vector $\hat{k}_i=k_i/k$. The polarization vectors are generated from x and y direction unit vectors as $\epsilon_\pm^i(\mathbf{k})=\frac{1}{\sqrt{2}}(e_x^i\pm\mathrm{i}e_y^i)$, based on which polarization tensors read $e_{ij}^{\pm}(\mathbf{k})=\epsilon_i^{\pm}(\mathbf{k})\otimes\epsilon_j^{\pm}(\mathbf{k})$ and $\epsilon_3^i=\hat{k}^i$. It is clear that it holds the relations (contraction over repeated indexes)

$$k^i\epsilon_i^{\pm}=0,\quad \eta_{ijk}k^j\hat{\epsilon}_\pm^k=\mp\mathrm{i}k\hat{\epsilon}_i^{\pm},\quad \epsilon_i^{\pm}\epsilon_\pm^i=0,\quad \epsilon_i^{\pm}\epsilon_\mp^i=1, \tag{B2}$$

$$\delta_{ij}e_{ij}^{\pm}(\mathbf{k})=P_{ij}(\mathbf{k})e_{ij}^{\pm}(\mathbf{k})=0,\quad P_{im}(\mathbf{k})\epsilon_m^\lambda(\mathbf{k})=\epsilon_i^\lambda, \tag{B3}$$

and

$$\sum_\lambda \epsilon_i^\lambda (\epsilon_j^\lambda)^* = \delta_{ij}, \quad \sum_\lambda \lambda \epsilon_i^\lambda (\epsilon_j^\lambda)^* = (\sigma_2)_{ij} = -\mathrm{i}\eta_{ij3}, \tag{B4}$$

where σ_2 is the Pauli matrix along the y direction. Based on (B3), it also yields

$$\Pi_{ij,mn}(\mathbf{k}) e_{ij}^\lambda(\mathbf{k}) = e_{mn}^\lambda(\mathbf{k}), \quad P_{ij}(\mathbf{k}) P_{ij}(\mathbf{p}) = \cos\theta. \tag{B5}$$

Then the summation over polarization state λ of two polarized vectors is

$$\begin{aligned}\sum_{\lambda=\pm} \epsilon_\lambda^{m_1} (\epsilon_\lambda^{m_2})^* C_\lambda &= \sum_{\lambda=\pm} \epsilon_\lambda^{m_1} (\epsilon_\lambda^{m_2})^* \frac{1}{2}(C_\lambda + C_{\bar\lambda}) \\ &\quad + \sum_{\lambda=\pm} \epsilon_\lambda^{m_1} (\epsilon_\lambda^{m_2})^* \frac{1}{2}(C_\lambda - C_{\bar\lambda}) \\ &= \frac{1}{2}(C_+ + C_-) \sum_{\lambda=\pm} \epsilon_\lambda^{m_1} (\epsilon_\lambda^{m_2})^* \\ &\quad + \frac{1}{2}(C_+ - C_-) \sum_{\lambda=\pm} \lambda \epsilon_\lambda^{m_1} (\epsilon_\lambda^{m_2})^* \\ &= \frac{1}{2}(C_+ + C_-)\delta^{m_1 m_2} + \frac{1}{2}(C_+ - C_-)(\sigma_2)^{m_1 m_2},\end{aligned} \tag{B6}$$

where C_λ is any complex variable dependent on polarization state λ and $\bar\lambda = -\lambda$.

The tensors could be written in the form of matrices:

$$\begin{aligned} e_{ij}^\pm(\mathbf{k}) &= \begin{pmatrix} 1 & \pm\mathrm{i} & 0 \\ \pm\mathrm{i} & -1 & 0 \\ 0 & 0 & 0 \end{pmatrix}, \\ \hat p_i \hat p_j &= \begin{pmatrix} \hat p_x^2 & \hat p_x \hat p_y & \hat p_x \hat p_z \\ \hat p_x \hat p_y & \hat p_y^2 & \hat p_y \hat p_z \\ \hat p_x \hat p_z & \hat p_y \hat p_z & \hat p_z^2 \end{pmatrix}, \\ \eta_{ijm}\hat k^m &= \begin{pmatrix} 0 & \hat k_3 & -\hat k_2 \\ -\hat k_3 & 0 & \hat k_1 \\ \hat k_2 & -\hat k_1 & 0 \end{pmatrix}. \end{aligned} \tag{B7}$$

In a spherical coordinate system, $\hat p^i$ read $p_x = \sin\theta\cos\varphi$, $p_y = \sin\theta\sin\varphi$, $p_z = \cos\theta$. Thus we obtain the following equations under contraction [36,37]:

$$e_{ij}^\pm(\mathbf{k}) \eta_{ijm} \hat p^m = e_{ij}^\pm \delta^{ij} = 0, \tag{B8}$$

$$\eta_{ijm}\hat p^m \eta_{ijn} \hat k^n = \hat p^m \hat k^m = \cos\theta, \tag{B9}$$

$$e_{ij}^\pm(\mathbf{k}) \hat p^i \hat p^j = (p_x \pm \mathrm{i} p_y)^2 = \mathrm{e}^{\pm \mathrm{i}2\varphi} \sin^2\theta, \tag{B10}$$

$$\epsilon_\lambda^i(\mathbf{k}) \epsilon_{\lambda'}^{m*}(\mathbf{k}) P_{im}(\mathbf{p}) = \delta_{\lambda\lambda'} - \frac{1}{2}\sin^2\theta e^{\mathrm{i}(\lambda-\lambda')\varphi}, \tag{B11}$$

$$\epsilon_\lambda^i(\mathbf{k}) \epsilon_{\lambda'}^{m*}(\mathbf{k}) \hat p_i \hat p_m = \frac{1}{2}\sin^2\theta \mathrm{e}^{\mathrm{i}(\lambda-\lambda')\varphi}, \tag{B12}$$

$$\mathrm{i}\epsilon_\lambda^i(\mathbf{k}) \epsilon_{\lambda'}^{m*}(\mathbf{k}) \eta_{imj} \hat p^j = \cos\theta(1 - \delta_{\lambda\lambda'}). \tag{B13}$$

APPENDIX C: DERIVATION OF EQS. (41) AND (42)

Starting from Friedmann-Robertson-Walker equation (3) in term of cosmic time t, the equation of motion of axion ϕ from Eq. (40) in coordinate space reads

$$\left[\frac{\mathrm{d}^2}{\mathrm{d}t^2} + 3H - \partial^i\partial_i + V_{,\phi}\right]\phi = \frac{\alpha_c}{f}\hat E_i(\mathbf{x}, t)\hat B_i(\mathbf{x}, t), \tag{C1}$$

where $V_{,\phi}$ denotes the derivative of potential $V(\phi)$ with respect to field ϕ, i.e., $\mathrm{d}V/\mathrm{d}\phi$. Axion inflaton could be composed into three parts, the quantum background ϕ_0, the quantum fluctuation $\delta\phi_\mathrm{q}$, and the thermal fluctuation $\delta\phi_\mathrm{T}$. Following the main idea of the present paper that gauge fields perturb the inflaton via thermal effects, ϕ_0 and $\delta\phi_\mathrm{q}$ are treated as the normal case in cold inflation by equations without sources while the equation of $\delta\phi_\mathrm{T}$ is perturbed by the thermal gauge fields. Then we obtain three equations about axion inflaton in momentum space:

$$\left[\frac{\mathrm{d}^2}{\mathrm{d}t^2} + 3H + V_{,\phi}\right]\phi_0 = 0; \tag{C2a}$$

$$\left[\frac{\mathrm{d}^2}{\mathrm{d}t^2} + 3H + \frac{k^2}{a^2} + V_{,\phi\phi}\right]\delta\phi_\mathrm{q} = 0; \tag{C2b}$$

and

$$\begin{aligned}&\left[\frac{\mathrm{d}^2}{\mathrm{d}t^2} + 3H + \frac{k^2}{a^2} + V_{,\phi\phi}\right]\delta\phi_\mathrm{T} \\ &\quad = \frac{\alpha_c}{f}\int \frac{d^3p}{(2\pi)^3}\hat E_i(\mathbf{k}-\mathbf{p}, t)\hat B_i(\mathbf{p}, t).\end{aligned} \tag{C2c}$$

Substituting the definition of conformal time $\mathrm{d}\tau = \mathrm{d}t/a$ into Eq. (C2c), it arrives as

$$\begin{aligned}&\left[\frac{\mathrm{d}^2}{\mathrm{d}\tau^2} + k^2 + a^2 V_{,\phi\phi} - \frac{a''}{a}\right](a\delta\phi_\mathrm{T}) \\ &\quad = a^3\frac{\alpha_c}{f}\int \frac{d^3p}{(2\pi)^3}\hat E_i(\mathbf{k}-\mathbf{p}, \tau)\hat B_i(\mathbf{p}, \tau).\end{aligned} \tag{C3}$$

For later convenience of expression, we omit the subscript T marked in Eq. (C3) and $\delta\phi$ specifically refers to the thermal perturbation in this paper. If neglecting the contribution of slow-roll approximations, namely $a = -1/(H\tau)$, $V_{,\phi\phi}/H^2 \sim 0$, and $a''/a = 2/\tau^2$, we have the leading order of Eq. (C3) as shown in Eq. (41).

Tensor fluctuation perturbed from thermal gauge fields could be obtained by Einstein equation

$$\left[\frac{\mathrm{d}^2}{\mathrm{d}t^2}+3H+\frac{k^2}{a^2}\right]\hat{h}_{ij}=16\pi G\Pi_{ij}^{mn}(\mathbf{k})\hat{T}_{mn}(\mathbf{k},t), \quad \text{(C4)}$$

where $\Pi_{ij}^{mn}(\mathbf{k})$ is the transverse traceless operator along direction $\mathbf{k}$ with symmetric contraction relation $g_{mn}\Pi_{ij}^{mn}=0$ and $\hat{T}_{mn}(\mathbf{k},\tau)$ is the energy-momentum tensor of the primordial electromagnetic field that appeared in Eq. (20). Repeating the calculations about thermal sourced scalar perturbation, we get the motion of equation of sourced tensor perturbation in terms of conformal time, which is shown in Eq. (42).

APPENDIX D: DETAILS ON THE CALCULATIONS OF SCALAR CORRELATOR

The computation of the scalar correlator starts from Eq. (47) at the superhorizon limit, and the second term in Eq. (48) reads (contraction over repeated indexes)

$$\begin{aligned}
&\left\langle\hat{E}_i(\mathbf{k}-\mathbf{p},\eta_1)\hat{E}_j(\mathbf{k}'-\mathbf{p},\eta_2)\right\rangle\left\langle\hat{B}_i(\mathbf{p},\eta_1)\hat{B}_j(\mathbf{q},\eta_2)\right\rangle\\
&\propto n_{\mathrm{B}}(\omega_{|\mathbf{k}-\mathbf{p}|}/aT)n_{\mathrm{B}}(\omega_p/aT)\cdot\left[\left(\delta_{ij}-(\widehat{k-p})_i(\widehat{k-p})_j\right)|\mathbf{k}-\mathbf{p}|^2P_E(|\mathbf{k}-\mathbf{p}|,\tau)-\mathrm{i}\eta_{ijm}(\widehat{k-p})^m|\mathbf{k}-\mathbf{p}|^2S_E(|\mathbf{k}-\mathbf{p}|,\tau)\right]\\
&\quad\cdot[(\delta_{ij}-\hat{p}_i\hat{p}_j)p^2P_B(p,\tau)+\mathrm{i}\eta_{ijn}\hat{p}^np^2S_B(p,\tau)]=n_{\mathrm{B}}(\omega_{|\mathbf{k}-\mathbf{p}|}/aT)n_{\mathrm{B}}(\omega_p/aT)|\mathbf{k}-\mathbf{p}|^2p^2\\
&\quad\cdot\left\{\left[1+(\widehat{k-p})_i\hat{p}^i(\widehat{k-p})_j\hat{p}^j\right]P_E(|\mathbf{k}-\mathbf{p}|,\tau)P_B(p,\tau)+(\widehat{k-p})_i\hat{p}^iS_E(|\mathbf{k}-\mathbf{p}|,\tau)S_B(p,\tau)\right\}\\
&=n_{\mathrm{B}}(\omega_{|\mathbf{k}-\mathbf{p}|}/aT)n_{\mathrm{B}}(\omega_p/aT)p^2[(2p^2+k^2-4pk\cos\theta)P_EP_B+2(p-k\cos\theta)|\mathbf{k}-\mathbf{p}|S_ES_B]\\
&=2n_{\mathrm{B}}(\omega_{|\mathbf{k}-\mathbf{p}|}/aT)n_{\mathrm{B}}(\omega_p/aT)p^4[P_E(p,\tau)P_B(p,\tau)+S_E(p,\tau)S_B(p,\tau)]+\mathcal{O}(k\cos\theta,k^2). \quad \text{(D1)}
\end{aligned}$$

Now recall Eq. (49). Define $z_1=-k\eta_1$, $z_2=-k\eta_2$, $\cos\theta=\hat{p}_i\hat{k}^i$, $x=p/aH$, and $\tilde{k}_p=k/aH$,

$$\begin{aligned}
\left\langle\hat{\mathcal{R}}(\mathbf{k},\tau)\hat{\mathcal{R}}(\mathbf{k}',\tau)\right\rangle=4\left(\frac{H^2}{\dot{\phi}}\right)^2\left(\frac{\alpha_cM_p}{f}\right)^2\left(\frac{H}{M_p}\right)^2\frac{1}{k^3}\delta^3(\mathbf{k}+\mathbf{k}')\int_0^\infty\mathrm{d}z_2\,\frac{\sin z_2-z_2\cos z_2}{z_2^5}\mathrm{e}^{-(\Gamma/k)z_2}\\
\times\int_0^{z_2}\mathrm{d}z_1(\sin z_1-z_1\cos z_1)\mathrm{e}^{(\Gamma/k)z_1}\cdot2\pi\int_0^\pi\mathrm{d}\theta\sin\theta\int_0^\infty\mathrm{d}x x^6\\
\times\{n_{\mathrm{B}}(\omega_{|\mathbf{k}-\mathbf{p}|}/aT)n_{\mathrm{B}}(x)[P_B(x)P_E(x)+S_B(x)S_E(x)]+n_{\mathrm{B}}^2(x)[P_c^2(x)+S_c^2(x)]\}. \quad \text{(D2)}
\end{aligned}$$

We first calculate the integral including $n_{\mathrm{B}}(|\mathbf{k}-\mathbf{p}|)$ for condition $4\mu^2<1$:

$$\begin{aligned}
I_1^s(4\mu^2<1)&=\int_0^\pi\mathrm{d}\theta\sin\theta\int_0^\infty\mathrm{d}x x^6n_{\mathrm{B}}(\omega_{|\mathbf{k}-\mathbf{p}|}/aT)n_{\mathrm{B}}(x)[P_B(x)P_E(x)+S_B(x)S_E(x)]\\
&=\int_0^\pi\mathrm{d}\theta\sin\theta\int_0^\infty\mathrm{d}x x^6\sum_{n=1}^\infty\sum_{m=1}^\infty\mathrm{e}^{-n(H/T)\sqrt{x^2-2x\cdot\tilde{k}_p\cos\theta+\tilde{k}_p^2+\mu^2}}\mathrm{e}^{-m(H/T)x}[P_B(x)P_E(x)+S_B(x)S_E(x)]\\
&\approx2\int_0^\infty\mathrm{d}x x^6\sum_{n=1}^\infty\sum_{m=1}^\infty\mathrm{e}^{-(m+n)(H/T)x}\mathrm{e}^{-n(H/T)(\sqrt{\mu^2+\tilde{k}_p^2}-\tilde{k}_p)}[P_B(x)P_E(x)+S_B(x)S_E(x)]\\
&=\left(\frac{T}{H}\right)^{5-4\ell}\Gamma(5-4\ell)\left|\frac{(\ell+1)\Gamma^2(2\ell+2)}{(2\ell+1)^2\cdot2^{2\ell}}\right|^2\left(\frac{\mathrm{e}^{2\pi\xi}}{|\Gamma(\ell+1+\mathrm{i}\xi)|^4}+\frac{\mathrm{e}^{-2\pi\xi}}{|\Gamma(\ell+1-\mathrm{i}\xi)|^4}\right)\\
&\quad\cdot2\sum_{n=1}^\infty\zeta(5-4\ell,n+1)\mathrm{e}^{-n(H/T)(\sqrt{\mu^2+\tilde{k}_p^2}-\tilde{k}_p)}. \quad \text{(D3)}
\end{aligned}$$

In the second step of the equation above, series expansion

$$\frac{1}{\mathrm{e}^x-1}=\frac{\mathrm{e}^{-x}}{1-\mathrm{e}^{-x}}=\sum_{n=1}^\infty\mathrm{e}^{-nx} \quad \text{(D4)}$$

has been used. In the third step, integral Eq. (E5) and its approximation have been applied. In the fourth step, Eqs. (E8) and (E9), and electromagnetic correlators (27), (29), and (31) have been used. Since the series converges rapidly as $n > 1$, it is safe to keep only the first term in series at the superhorizon limit

$$\sum_{n=1}^{\infty}\sum_{m=1}^{\infty}\frac{1}{(m+n)^{5-4\ell}}\mathrm{e}^{-n(H/T)(\sqrt{\mu^2+\tilde{k}_p^2}-\tilde{k}_p)} \approx \frac{\mathrm{e}^{-\alpha_T}}{2^{5-4\ell}}. \tag{D5}$$

Similarly, the second integral in Eq. (D2) for $4\mu^2 < 1$ reads

$$\begin{aligned} I_2^s(4\mu^2<1) &= \int_0^{\pi}\mathrm{d}\theta\sin\theta\int_0^{\infty}\mathrm{d}x x^6 n_{\mathrm{B}}^2(x)[P_C^2(x)+S_C^2(x)] \\ &= 2\int_0^{\infty}\mathrm{d}x x^6\sum_{n=2}^{\infty} n\mathrm{e}^{-n(T/H)x}(P_c^2(x)+S_c^2(x)) = 2\left(\frac{T}{H}\right)^{5-4\ell}\Gamma(5-4\ell) \\ &\quad\cdot\left|\frac{(\ell+1)\Gamma^2(2\ell+2)}{(2\ell+1)^2\cdot 2^{2\ell}}\right|^2\left(\frac{\mathrm{e}^{2\pi\xi}}{|\Gamma(\ell+1+\mathrm{i}\xi)|^4}+\frac{\mathrm{e}^{-2\pi\xi}}{|\Gamma(\ell+1-\mathrm{i}\xi)|^4}\right)[\zeta(4-5\ell)-1] \end{aligned} \tag{D6}$$

and

$$\begin{aligned} I^s(4\mu^2>1) &= \int_0^{\pi}\mathrm{d}\theta\sin\theta\int_0^{\infty}\mathrm{d}x x^6\{n_{\mathrm{B}}(\omega_{|\mathbf{k}-\mathbf{p}|}/aT)n_{\mathrm{B}}(x)[P_B(x)P_E(x)+S_B(x)S_E(x)] \\ &\quad + n_{\mathrm{B}}(x)[P_c^2(x)+S_c^2(x)]\}_{4\mu^2>1} \approx 2\left(\frac{T}{H}\right)^7\Gamma(7)\left|\frac{(\ell+1)\Gamma^2(2\ell+2)}{(2\ell+1)^2\cdot 2^{2\ell}}\right|^2 \\ &\quad\cdot\left(\frac{\mathrm{e}^{2\pi\xi}}{|\Gamma(\ell+1+\mathrm{i}\xi)|^4}+\frac{\mathrm{e}^{-2\pi\xi}}{|\Gamma(\ell+1-\mathrm{i}\xi)|^4}\right)\left[\frac{\mathrm{e}^{\alpha_T}\mathrm{Li}_7(\mathrm{e}^{-\alpha_T})-\zeta(7)}{\mathrm{e}^{\alpha_T}-1}+\zeta(7)-1\right], \end{aligned} \tag{D7}$$

where $\mathrm{Li}_s(z)$ is the polylogarithm function [see Eq. (E10)]. Finally, from Eqs. (E1)–(E4), the double integral over z_1 and z_2 in Eq. (D2) reads

$$\int_0^{\infty}\mathrm{d}z_2\frac{\sin z_2 - z_2\cos z_2}{z_2^5}\mathrm{e}^{-(\Gamma/k)z_2}\int_0^{z_2}\mathrm{d}z_1(\sin z_1 - z_1\cos z_1)\mathrm{e}^{(\Gamma/k)z_1} \approx \begin{cases} \frac{\pi}{24}+\frac{\Gamma}{12k}(5-8\ln 2)+\mathcal{O}((\Gamma/k)^2), & \Gamma/k\ll 1, \\ \frac{\pi}{24}+\frac{1}{4}\frac{k}{\Gamma}+\mathcal{O}((k/\Gamma)^2), & \Gamma/k\gg 1. \end{cases} \tag{D8}$$

Substituting Eqs. (D3), (D6), and (D7) into Eq. (D2), we can get the two-point correlation function (50) sourced from thermal Abelian gauge fields.

APPENDIX E: INTEGRALS AND SPECIAL FUNCTIONS

The following integrals have been used in this paper:

$$\begin{aligned} \int_0^x(\sin y - y\cos y)\mathrm{e}^{ay}\mathrm{d}y &= \frac{2+\mathrm{e}^{ax}[-(2+ax+a^3x)\cos x+(a(a^2+3)-(a^2+1)x)\sin x]}{(a^2+1)^2} \\ &\approx \mathrm{e}^{ax}\begin{cases}(2-2\cos x - x\sin x)+a(-2x-x\cos x+3\sin x)+\mathcal{O}(a^2), & a\ll 1\\ (2-2\cos x - x\sin x)+\frac{1}{a}(\sin x - x\cos x)+\mathcal{O}(a^{-2}), & a\gg 1\end{cases}, \end{aligned} \tag{E1}$$

$$\int_0^{\infty}\mathrm{d}x\frac{(\sin x - x\cos x)^2}{x^5} = \frac{1}{4}, \tag{E2}$$

$$\int_0^\infty \mathrm{d}x x^{-5}(\sin x - x\cos x)(3\sin x - x\cos x - 2x) = \frac{1}{12}(5 - 8\ln 2), \tag{E3}$$

$$\int_0^\infty \mathrm{d}x x^{-5}(\sin x - x\cos x)(2 - 2\cos x - x\sin x) = \frac{\pi}{24}, \tag{E4}$$

$$\begin{aligned}&\int_0^\pi \mathrm{d}\theta \sin\theta \mathrm{e}^{-\sqrt{x^2-2kx\cos\theta+k^2+\mu^2}} \\ &= \frac{1}{kx}\left[\mathrm{e}^{-\sqrt{(x-k)^2+\mu^2}}\left(1+\sqrt{(x-k)^2+\mu^2}\right)\right. \\ &\quad \left. - \mathrm{e}^{-\sqrt{(x+k)^2+\mu^2}}\left(1+\sqrt{(x+k)^2+\mu^2}\right)\right] \\ &\approx 2\mathrm{e}^{-\mu}\mathrm{e}^{k-\sqrt{k^2+\mu^2}} + \mathcal{O}(k^2,\mu^2), \quad k \ll 1,\end{aligned} \tag{E5}$$

$$\begin{aligned}&\int_0^\pi \mathrm{d}\theta \sin\theta\cos\theta \mathrm{e}^{-\sqrt{x^2-2kx\cos\theta+k^2+\mu^2}} \\ &\approx -\frac{\mu^2}{3x}\mathrm{e}^{-x}\mathrm{e}^{-(\sqrt{k^2+\mu^2}-k)}, \quad \mu^2 \ll 1,\end{aligned} \tag{E6}$$

and

$$\int_0^{+\infty} \mathrm{d}z_3 \frac{\sin z_3 - z_3\cos z_3}{z_3^7}\int_0^{z_3}\mathrm{d}z_2(\sin z_2 - z_2\cos z_2) \times \int_0^{z_2}\mathrm{d}z_1(\sin z_1 - z_1\cos z_1) = \frac{17\pi}{2880}. \tag{E7}$$

An integral related to the Gamma function is

$$\int_0^{+\infty}\mathrm{d}x x^{s-1}\mathrm{e}^{-ax} = a^{-s}\Gamma(s), \tag{E8}$$

and the Hurwitz zeta function is defined as [24]

$$\zeta(s,a) = \sum_{m=0}^{\infty}\frac{1}{(m+a)^s}. \tag{E9}$$

The polylogarithm function is expressed as

$$\mathrm{Li}_s(z) = \sum_{n=1}^{\infty}\frac{z^n}{n^s}. \tag{E10}$$

[1] A. Berera, I. G. Moss, and R. O. Ramos, Warm inflation and its microphysical basis, Rep. Prog. Phys. **72**, 026901 (2009).
[2] V. Kamali, M. Motaharfar, and R. O. Ramos, Recent developments in warm inflation, Universe **9**, 124 (2023).
[3] A. Salvio, A. Strumia, and W. Xue, Thermal axion production, J. Cosmol. Astropart. Phys. 01 (2014) 011.
[4] K. Freese, J. A. Frieman, and A. V. Olinto, Natural inflation with pseudo Nambu-Goldstone bosons, Phys. Rev. Lett. **65**, 3233 (1990).
[5] N. K. Stein and W. H. Kinney, Natural inflation after Planck 2018, J. Cosmol. Astropart. Phys. 01 (2022) 022.
[6] B. A. Bassett, S. Tsujikawa, and D. Wands, Inflation dynamics and reheating, Rev. Mod. Phys. **78**, 537 (2006).
[7] R. Z. Ferreira and A. Notari, Thermalized axion inflation: Natural and monomial inflation with small r, Phys. Rev. D **97**, 063528 (2018).
[8] O. Wantz and E. P. S. Shellard, Axion cosmology revisited, Phys. Rev. D **82**, 123508 (2010).
[9] R. Sharma, S. Jagannathan, T. R. Seshadri, and K. Subramanian, Challenges in inflationary magnetogenesis: Constraints from strong coupling, backreaction, and the Schwinger effect, Phys. Rev. D **96**, 083511 (2017).
[10] R. J. Z. Ferreira, R. K. Jain, and M. S. Sloth, Inflationary magnetogenesis without the strong coupling problem, J. Cosmol. Astropart. Phys. 10 (2013) 004.
[11] R. J. Z. Ferreira, R. K. Jain, and M. S. Sloth, Inflationary magnetogenesis without the strong coupling problem II: Constraints from CMB anisotropies and B-modes, J. Cosmol. Astropart. Phys. 06 (2014) 053.
[12] N. Barnaby, R. Namba, and M. Peloso, Phenomenology of a pseudo-scalar inflaton: Naturally large nongaussianity, J. Cosmol. Astropart. Phys. 04 (2011) 009.
[13] N. Barnaby, E. Pajer, and M. Peloso, Gauge field production in axion inflation: Consequences for monodromy, non-Gaussianity in the CMB, and gravitational waves at interferometers, Phys. Rev. D **85**, 023525 (2012).
[14] O. Özsoy, Parity violating non-Gaussianity from axion-gauge field dynamics, Phys. Rev. D **104**, 123523 (2021).
[15] R. Z. Ferreira and A. Notari, Thermalized axion inflation, J. Cosmol. Astropart. Phys. 09 (2017) 007.
[16] X. B. Li and Y. L. Wu, Thermodynamics of warm axionic Abelian gauge inflation, Chin. Phys. B **32**, 119801 (2023).
[17] N. Barnaby and M. Peloso, Large non-Gaussianity in axion inflation, Phys. Rev. Lett. **106**, 181301 (2011).
[18] O. Ozsoy, On synthetic gravitational waves from multi-field inflation, J. Cosmol. Astropart. Phys. 04 (2018) 062.
[19] R. Z. Ferreira and A. Notari, Observable windows for the QCD axion through the number of relativistic species, Phys. Rev. Lett. **120**, 191301 (2018).
[20] R. Sharma, K. Subramanian, and T. R. Seshadri, Gravitational wave generation in a viable scenario of inflationary magnetogenesis, Phys. Rev. D **101**, 103526 (2020).
[21] E. Masso, F. Rota, and G. Zsembinszki, Axion thermalization in the early universe, Phys. Rev. D **66**, 023004 (2002).

[22] R. Sharma, K. Subramanian, and T. R. Seshadri, Generation of helical magnetic field in a viable scenario of inflationary magnetogenesis, Phys. Rev. D **97**, 083503 (2018).
[23] E. W. Kolb and M. S. Turner, *The Early Universe*, Frontiers in Physics Vol. 69 (Addison-Wesley, Redwood City, CA, 1990), p. 547.
[24] F. W. J. Olver, D. W. Lozier, R. F. Boisvert *et al.*, *NIST Handbook of Mathematical Functions* (Cambridge University Press, Cambridge, England, 2010).
[25] T. Kobayashi, Primordial magnetic fields from the post-inflationary universe, J. Cosmol. Astropart. Phys. 05 (2014) 040.
[26] Y. Qiu and L. Sorbo, Spectrum of tensor perturbations in warm inflation, Phys. Rev. D **104**, 083542 (2021).
[27] X. B. Li, H. Wang, and J. Y. Zhu, Gravitational waves from warm inflation, Phys. Rev. D **97**, 063516 (2018).
[28] G. D. Mahan, *Many-Particle Physics* (Springer Science & Business Media, New York, 2000).
[29] T. Kobayashi and H. Afshordi, Schwinger effect in 4D de Sitter space and constraints on magnetogenesis in the early universe, J. High Energy Phys. 10 (2014) 166.
[30] R. O. Ramos and L. A. D. Silva, Power spectrum for inflation models with quantum and thermal noises, J. Cosmol. Astropart. Phys. 03 (2013) 032.
[31] S. Bartrum, M. Bastero-Gil, A. Berera, R. Cerezo, R. O. Ramos, and J. G. Rosa, The importance of being warm (during inflation), Phys. Lett. B **732**, 116 (2014).
[32] M. Benetti and R. O. Ramos, Warm inflation dissipative effects: Predictions and constraints from the Planck data, Phys. Rev. D **95**, 023517 (2017).
[33] M. Bastero-Gil, A. Berera, R. O. Ramos, and J. G. Rosa, Towards a reliable effective field theory of inflation, Phys. Lett. B **813**, 136055 (2021).
[34] K. V. Berghaus, P. W. Graham, and D. E. Kaplan, Minimal warm inflation, J. Cosmol. Astropart. Phys. 03 (2020) 034.
[35] A. Dzieciol, S. Yngve, and P. O. Fröman, Coulomb wave functions with complex values of the variable and the parameters, J. Math. Phys. (N.Y.) **40**, 6145 (1999).
[36] A. Buonanno, Gravitational waves, arXiv:0709.4682.
[37] M. Maggiore, *Gravitational Waves (Volume 1): Theory and Experiments* (Oxford University Press, Oxford, 2007).